

Unsupervised Deep Transfer Learning for Intelligent Fault Diagnosis: An Open Source and Comparative Study

Zhibin Zhao^{a,b}, Qiyang Zhang^a, Xiaolei Yu^a, Chuang Sun^a, Shibin Wang^a, Ruqiang Yan^{a,*}, Xuefeng Chen^a

^a*School of Mechanical Engineering, Xi'an Jiaotong University, Xi'an, China*

^b*Centre for Health Informatics, University of Manchester, Manchester, United Kingdom*

Abstract

Recent progress on intelligent fault diagnosis has greatly depended on the deep learning and plenty of labeled data. However, the machine often operates with various working conditions or the target task has different distributions with the collected data used for training (we called the domain shift problem). This leads to the deep transfer learning based (DTL-based) intelligent fault diagnosis which attempts to remit this domain shift problem. Besides, the newly collected testing data are usually unlabeled, which results in the subclass DTL-based methods called unsupervised deep transfer learning based (UDTL-based) intelligent fault diagnosis. Although it has achieved huge development in the field of fault diagnosis, a standard and open source code framework and a comparative study for UDTL-based intelligent fault diagnosis are not yet established. In this paper, commonly used UDTL-based algorithms in intelligent fault diagnosis are integrated into a unified testing framework and the framework is tested on five datasets. Extensive experiments are performed to provide a systematically comparative analysis and the benchmark accuracy for more comparable and meaningful further studies. To emphasize the importance and reproducibility of UDTL-based intelligent fault diagnosis, the testing framework with source codes will be released to the research community to facilitate future research. Finally, comparative analysis of results also reveals some open and essential issues in DTL for intelligent fault diagnosis which are rarely studied including transferability of features, influence of backbones, negative transfer, and physical priors. In summary, the released framework and comparative study can serve as an extended interface and the benchmark results to carry out new studies on UDTL-based intelligent fault diagnosis. The code framework is available at <https://github.com/ZhaoZhibin/UDTL>.

Keywords: Unsupervised deep transfer learning, intelligent fault diagnosis, open source study

1. Introduction

With the rapid development of industrial big data and Internet of things in the Industry 4.0 background, Prognostic and Health Management (PHM) for industrial equipment is becoming increasingly important, leading to more and more intelligent maintenance systems for industrial equipment. Intelligent fault diagnosis is becoming an important branch in the machine PHM technology, and traditional machine learning methods, including support vector machine (SVM), and artificial neural network (ANN), have been widely applied in this field. While, with the increment of available data, data-driven intelligence methods with the ability for representation learning become increasingly popular. Under this background, Deep Learning (DL) [1] with advantages for adaptive feature extraction and pattern recognition of data

*Corresponding author

Email address: zhibinzhao1993@gmail.com (Zhibin Zhao)

processing gradually becomes a hot research focus for PHM of industrial equipment. Effectiveness of DL models, such as Convolutional Neural Network (CNN) [2], Deep Belief Network (DBN) [3], Sparse Autoencoder (SAE) [4], etc. for tasks in PHM has been validated successfully in current research.

Besides, effectiveness of DL for intelligent fault diagnosis is based on the following two assumptions: 1) plenty of labeled data are available; 2) fault patterns of training datasets in source domain are the same as those of testing datasets in the target domain (mathematically, the training datasets (the source domain) should follow the same distribution with the testing datasets (the target domain)). The labeled data can be collected for model training by the fault seeding or simulations in the laboratory. However, training datasets acquired in the laboratory are not strictly consistent with the data generated in real industrial equipment. If DL models are trained using these datasets, they might overfit the training datasets, which leads to a weak generalization for real industrial applications, especially for the new conditions that are not trained in models. Besides, the machine often operates with various working conditions in the real application, which requires trained models adaptive to the change of working conditions. These two aspects make models trained in the source domain hard to be generalized or transferred to the target domain, directly. Common characteristics existing in the data from these two domains due to the intrinsic similarity in different application scenarios or different working conditions make this domain shift manageable. Hence, to let DL models trained in the source domain work well in the target domain, an effective way is to fine-tune DL models with a few labeled data in the target domain, and then the fine-tuned model can be used to diagnose new data in the target domain and this way is also called deep transfer learning-based (DTL-based) intelligent fault diagnosis. However, the newly collected engineering data or the data under different working conditions are usually unlabeled and it is sometimes very difficult, or even impossible to label these data. Therefore, it is necessary to investigate the unsupervised version of DTL which means that there is no labeled data in the target domain, and in this paper, we mainly focus on this kind version called unsupervised deep transfer learning-based (UDTL-based) intelligent fault diagnosis.

UDTL is widely used and has achieved huge development in the field of computer vision (CV) and natural language processing (NLP), due to the application value, open source codes, and the baseline accuracy in these fields. But there are little open source codes or the baseline accuracy in the field of UDTL-based intelligent fault diagnosis, plenty of research has been published on UDTL-based intelligent fault diagnosis by simply using models that already have been published in other fields. Due to the lack of open source codes, the results in these published papers are very hard to repeat for further comparisons. This is not beneficial to identify the state-of-the-art methods in this field, and furthermore, it is unfavorable to the advancement of this field on a long view. Hence, it is very important to perform a comparative study, provide a baseline accuracy, and release open source codes of UDTL-based algorithms which are widely applied to intelligent fault diagnosis. More importantly, open source codes are essential to finding existing problems and potential improvement directions of these algorithms for the research community in this field.

For testing UDTL-based algorithms, the unified testing framework, parameter setting, and datasets are three important aspects to affect fairness and effectiveness of comparisons between different algorithms. While, due to the leak of open source codes, which causes the inconsistency of these factors, there are a lot of unfair and unsuitable comparisons in UDTL-based algorithms leading to exist some similar studies and ineffective improvement in the current research, which is harmful to the development of advanced algorithms. It seems that researchers are continuing to combine the new algorithms which have already been published in the field of DTL, and the proposed algorithms always have better

performance than the former algorithms, which comes to the questions: Is the improvement beneficial to intelligent fault diagnosis or just depends on the excessive parameter adjustment? However, the open and essential issues in DTL for intelligent fault diagnosis are rarely studied, such as transferability of the features, influence of backbones, which transfer learning method works better, etc.

To fill in this gap, commonly used UDTL-based algorithms in intelligent fault diagnosis are integrated into a unified testing framework and tested on five datasets, in this paper. The UDTL-based intelligent diagnosis methods discussed in this study mainly consist of four kinds of methods: network-based DTL, instanced-based DTL, mapping-based DTL, and adversarial-based DTL. This testing framework with source codes will be released to the research community to facilitate the research on DTL for intelligent fault diagnosis. With this comparative study and open source codes, the authors try to give a benchmark (it is worth mentioning that results are just a lower bound of the accuracy) performance of current algorithms and attempt to find the core that determines the transfer performance of the algorithms.

The main contributions of this paper are summarized as follows:

- 1) *Various datasets and data splitting.* We collect most of the publicly available datasets which are suitable for UDTL-based intelligent fault diagnosis and provide a detailed discussion about its adaptability. We also discuss the way of data splitting and explain that it is more appropriate to split data into training and testing datasets regardless of whether they are in the source domain or in the target domain.
- 2) *Benchmark accuracy and further discussion.* We evaluate various UDTL-based intelligent diagnosis methods including network-based DTL, instanced-based DTL, mapping-based DTL, and adversarial-based DTL for different datasets and provide a systematic and comparative analysis and the benchmark accuracy (it is worth mentioning that the results are just a lower bound of accuracy) from several perspectives to make the future studies in this field more comparable and meaningful. We also discuss the transferability of features, influence of backbones, negative transfer, and other potential studies and applications.
- 3) *Open source codes.* To emphasize the importance and reproducibility of UDTL-based intelligent fault diagnosis, we release the whole evaluation codes framework that implements all the UDTL-based methods discussed in this paper under a unified interface for the advancement of this field. Meanwhile, This is an extensible framework that retains an extended interface for everyone to combine different algorithms and load their own datasets to carry out new studies. The code framework is available at <https://github.com/ZhaoZhibin/UDTL>.

The rest of this paper is organized as follows: Section 2 provides a brief review of UDTL-based intelligent fault diagnosis. Evaluation algorithms, applications, datasets, data preprocessing and splitting, and evaluation methodology are introduced in Section 3 to 7. After that, in Section 8 and 9, evaluation results and further discussions are investigated, followed by the conclusion part in Section 10.

2. Brief Review

Transfer learning, which is a well-known tool to solve the problem of limited labeled data or no labeled data in the target domain, has developed rapidly in the field of artificial intelligence. Pan et al. [5] and Weiss et al. [6] reviewed the basic progress and various applications of transfer learning in 2009 and 2016, respectively. Recently, due to the strong

presentation ability of DL, it can learn more transferable features without any request of hand-craft features. Therefore, DTL (transfer learning methods based on DL models) has emerged as a popular branch and achieved many inspiring results, and researchers can refer to some excellent survey papers of DTL [7, 8]. Intelligent fault diagnosis is a natural transfer learning problem because of changes in working conditions and the lack of labeled fault data. Many traditional transfer learning methods have been applied to fault diagnosis research works, such as transfer component analysis (TCA) based models [9], subspace learning-based methods [10]. Since this paper mainly focuses on the application of DTL in the field of intelligent fault diagnosis, the following part will mainly review DTL-based intelligent fault diagnosis.

According to Tan et al. [7], DTL methods can be classified into four categories: network-based DTL, instanced-based DTL, mapping-based DTL, and adversarial-based DTL. In the following space, a brief review of DTL in intelligent fault diagnosis is summarized according to those four categories (for more detailed information, researchers can refer to two excellent reievew papers [11, 12] published recently).

Network-based DTL: Network-based DTL means that partial network parameters pre-trained in the source domain are transferred to be partial network parameters of the testing procedure or network parameters are fine-tuned with a few labeled data in the target domain. Pre-trained deep neural networks with the source data were used in [13–22] by freezing its partial parameters, and then part of network parameters were transferred to the target network and other parameters were fine-tuned with a small amount of target data. Pre-trained deep neural networks on ImageNet were used in [23–28] and were fine-tuned with limited target data to adapt the domain of engineer applications. Qureshi et al. [29] pre-trained nine deep sparse auto-encoders on a wind farm, and predictions on other wind farm datasets were taken by fine-tuning the pre-trained networks. Zhong et al. [30] trained CNN on enough normal samples and then replaced fully-connected layers with support vector machine (SVM) as the target model to train and test on fewer fault samples. Han et al. [31] discussed and compared three fine-tuning strategies: only fine-tuning the classifier, fine-tuning the feature descriptor and fine-tuning both the feature descriptor and the classifier for diagnosing unseen machine conditions. Besides, Xu et al. [32] pre-trained the offline CNN on the source domain and directly transferred them to the shallow layers of the online CNN with fine-tuning the online CNN on the target domain for online fault diagnosis.

Instanced-based DTL: Instanced-based DTL refers to reweight instances in the source domain to assist the classifier to predict on the target domain or use the statistics of instances in the target domain to help align the domains, such as TrAdaBoost [33] and adaptive Batch Normalization (AdaBN) [34]. Xiao et al. [35] used TrAdaBoost to enhance the diagnostic capability of the fault classifier by adjusting the weight factor of each training sample. Zhang et al. [36] and Qian et al. [37] used AdaBN to improve the domain adaptation ability of the model by ensuring that each layer receives data from a similar distribution.

Mapping-based DTL: Mapping-based DTL refers to map instances from both source and target domains to a feature space through deep neural network. In this feature space, the domain divergence is minimized by distance metrics such as correlation alignment (CORAL) [38], maximum mean discrepancy (MMD) [39, 40], multi kernels MMD (MK-MMD) [41, 42], joint distribution adaptation (JDA) [43], balanced distribution adaptation (BDA) [44], and Joint Maximum Mean Discrepancy (JMMD) [45]. Wang et al. [46] used BDA to adaptively balance the importance of the marginal and conditional distribution discrepancy between feature domains learned by deep neural networks for the power data analysis. Wang et al. [47] minimized the CORAL loss for reducing the marginal and conditional distribution discrepancy between domains in the feature space for fault diagnosis of a thermal system. Another metric distance called MMD

was widely used in the field of intelligent diagnosis [48–54], and Tong et al. [55, 56] reduced marginal and conditional distributions simultaneously across domains based on MMD in feature space by refining pseudo testing labels for bearing fault diagnosis. MK-MMD was used in [57–60] to better shift the distribution of learned features in the source domain to that in the target domains for intelligent fault classification. Han et al. [61] and Qian et al. [62] used JDA to align both conditional and marginal distributions of two datasets simultaneously to construct a more effective and robust feature representation for substantial distribution difference. Qian et al. [37] proposed the HKL divergence to adjust domain distributions further by aligning the high-order moments of distributions in source and target domains.

Adversarial-based DTL Adversarial-based DTL refers to an adversarial method using a domain discriminator to reduce the feature distribution discrepancy of source and target domains produced by the deep feature extractor [63, 64]. In [65–68], the source deep feature extractor was pre-trained with the labeled data and was used to generate target features. After that, features from both source and target domains were trained to maximize the domain discriminator loss which makes the source and target domains have similar distributions. Cheng et al. [69] utilized the Wasserstein distance to learn domain-invariant representations between two different feature distributions through adversarial training. Besides, another strategy using adversarial-based methods contains adopting the generative adversarial net (GAN) to generate samples for the target domain. For example, Xie et al. [70] trained cycle-GAN with the known condition to generate new samples for the unknown condition which only has one category and then used these new samples to train a classifier for intelligent fault diagnosis.

While a large number of DTL methods have been proposed in the field of intelligent fault classification, almost all the papers did not provide the source codes for other researchers to compare and improve. As discussed in the introduction section, open source codes are very important for intelligent fault diagnosis in both academic studies and engineer applications. To bridge this gap, this paper mainly realizes some existed algorithms about DTL in a unified code framework and uses the established framework to test some publicly available datasets in the field of fault diagnosis. More importantly, we release the source codes to contribute efforts to further research about DTL in intelligent fault diagnosis, especially for UDTL-based methods.

3. Evaluation Algorithm

In this section, we briefly introduce the definition of UDTL and the structure of the backbone. Then, UDTL-based intelligent diagnosis methods, including network-based DTL, instanced-based DTL, mapping-based DTL, and adversarial-based DTL are described in detailed.

3.1. The Definition of UDTL

First of all, to briefly describe the definition of UDTL, we must introduce some basic terms and symbols. In UDTL, it is assumed that labels in the source domain are all available, and the source domain can be defined as follows:

$$\mathcal{D}_s = \left\{ (x_i^s, y_i^s) \right\}_{i=1}^{n_s} \quad x_i^s \in X_s, y_i^s \in Y_s \quad (1)$$

where \mathcal{D}_s represents the source domain, $x_i^s \in \mathbb{R}^d$ is the i -th sample in the source domain, X_s is the union of all samples, y_i^s is the i -th label of the i -th sample, Y_s is the union of all different labels, and n_s means the total number of source samples.

In addition, it is assumed that labels in the target domain are unavailable, so the target domain can be defined as follows:

$$\mathcal{D}_t = \left\{ \left(x_i^t \right)_{i=1}^{n_t} \mid x_i^t \in X_t \right\} \quad (2)$$

where \mathcal{D}_t represents the target domain, $x_i^t \in \mathbb{R}^d$ is the i -th sample in the target domain, X_t is the union of all samples, and n_t means the total number of target samples.

The source and target domains follow the probability distributions P and Q , respectively. For UDTL, we hope to build a deep neural network which can classify the unlabeled samples in the target domain through learning the transferable features. It can be written as:

$$\hat{y} = \beta(x) \quad (3)$$

where $\beta(\cdot)$ represents a deep neural network and \hat{y} is the predicting result of the model. Thus, UDTL is aimed to minimize the target risk $\varepsilon_t(\beta)$ using the source data supervision [42].

$$\varepsilon_t(\beta) = \Pr_{(x,y) \sim Q} [\beta(x) \neq y] \quad (4)$$

Also, the total loss of UDTL can be written as

$$\mathcal{L} = \mathcal{L}_c + \lambda \mathcal{L}_{\text{UDTL}} \quad (5)$$

where \mathcal{L}_c is the softmax cross-entropy loss which measures the difference between predicted and true labels from the source domain shown in Eq. 6, λ is the trade-off parameter, and $\mathcal{L}_{\text{UDTL}}$ represents the partial loss to reduce the feature difference between the source and target domains.

$$\mathcal{L}_c = -\mathbb{E}_{(x_i^s, y_i^s) \in \mathcal{D}_s} \sum_{c=0}^{C-1} \mathbb{1}_{[y_i^s=c]} \log [\beta(x_i^s)] \quad (6)$$

where C is the number of all possible classes and $\mathbb{1}$ is the indicator function.

3.2. The Structure of Backbone

One of the most important parts of UDTL-based intelligent diagnosis is the structure of the backbone which acts as the role of feature extraction and has a huge impact on the testing accuracy. For example, in the field of image classification, different backbones, such as LeNet [71], AlexNet [2], VGG [72], GoogleNet [73], and ResNet [74], have different abilities of feature extraction and have led to different classification accuracies.

However, for UDTL-based intelligent fault diagnosis, different research works have their own backbones, and it is difficult to determine whose backbone is better. Therefore, direct comparisons with the results listed in other published papers are unfair and unsuitable due to different representative capacities of backbones. In this paper, we verify the performance of different UDTL-based intelligent diagnosis methods using the same CNN backbone to ensure a fair comparison.

As shown in Fig. 1, the CNN backbone consists of four one dimension (1D) convolutional layers that come with an 1D Batch Normalization (BN) layer and the ReLU activation function. Besides, the second combination comes with an

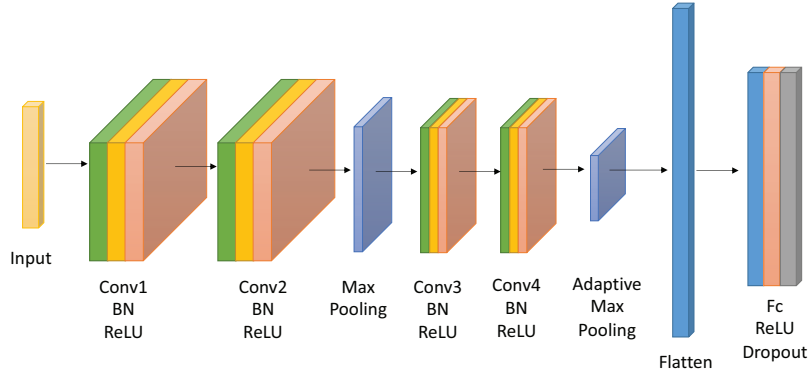


Fig. 1. The structure of the backbone.

Table 1: Parameters of the backbone.

Layers	Parameters
Conv1	out_channels=16, kernel_size=15
Conv2	out_channels=32, kernel_size=3
Max Pooling	kernel_size=2, stride=2
Conv3	out_channels=64, kernel_size=3
Conv4	out_channels=128, kernel_size=3
Adaptive Max Pooling	output_size=4
Fc	out_features=256
Dropout	p=0.5

Table 2: Parameters of the bottleneck layer.

Layers	Parameters
Fc	out_features=256
Dropout	p=0.5

1D Max Pooling layer to reduce parameters, and the fourth combination comes with an 1D Adaptive Max Pooling layer to realize the adaptation of the input length. The convolutional output is then flattened and passed through a fully-connected (Fc) layer, a ReLU activation function, and a Dropout layer. The detailed parameters are listed in Table 1 and the names of parameters are the same as names in Pytorch.

3.3. Network-based DTL

Network-based DTL means that partial network parameters pre-trained in the source domain are transferred to be partial network parameters of the testing procedure or network parameters are fine-tuned with a little labeled data in the target domain. The most popular network-based DTL method is to fine-tune the trained model utilizing a few labeled data in the target domain, and then the fine-tuned model can be used to test new data in the target domain directly. However, for UDTL-based intelligent diagnosis, labels in the target domain are unavailable. We use the backbone coming with a bottleneck layer (consisting of a Fc layer, a ReLU activation function, and a Dropout layer) and a basic Softmax classifier to construct our basic model (we call it Basis) which is shown in Fig. 2, and only samples from the source domain are used to train the model without any additional samples from the target domain. The trained model is used to test samples in the target domain directly, which means that source and target domains share the same model and parameters. Besides, parameters of the bottleneck layer are listed in Table 2.

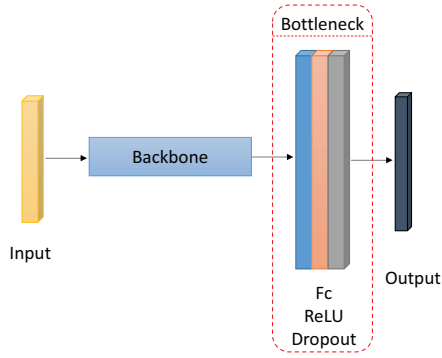


Fig. 2. The structure of the basic model.

3.4. Instanced-based DTL

Instanced-based DTL refers to reweight instances in the source domain to assist the classifier to predict labels in the target domain or use statistics of instances in the target domain to help align domains. In this paper, we use the method called AdaBN to represent one of instanced-based DTL methods and test the corresponding performance.

BN which can be used to avoid the issue of the internal covariate shifting is one of the most important techniques in CNN models. BN can lead to much faster training speed for CNN models than CNN without BN due to the fact that it makes the input distribution more stable. Detailed descriptions and properties can be referred to [75]. It is worth mentioning that BN layers are only updated in the training procedure and the global statistics of training samples are used to normalize testing samples during the test procedure.

AdaBN, which is a simple and parameter-free technique for the domain shift problem, was proposed in [34] to enhance the generalization ability of CNN models. The main idea of AdaBN is that during the testing phase, the global statistics of each BN layer are replaced with statistics in the target domain. In our AdaBN realization, after training, we provide two updating strategies to fine-tune the statistics of BN layers using target data, including updating through each batch and updating through the whole data. In this paper, we update statistics of BN layers through each batch considering the memory during the process.

3.5. Mapping-based DTL

Mapping-based DTL refers to map instances from both source and target domains to a feature space through deep feature extractor. There are many methods belonging to mapping instances in DTL, such as Euclidean distance, Minkowski distance, Kullback-Leibler, correlation alignment (CORAL) [38], maximum mean discrepancy (MMD) [39, 40], multi kernels MMD (MK-MMD) [41, 42], joint distribution adaptation (JDA) [43], balanced distribution adaptation (BDA) [44], and Joint Maximum Mean Discrepancy (JMMD) [45]. In this paper, we use MK-MMD, JMMD, and CORAL to represent the mapping-based method and test corresponding accuracies.

3.5.1. MK-MMD

To introduce the definition of MK-MMD, we briefly explain the concept of MMD. MMD was first proposed in [39] and was used in transfer learning by many other researchers [76, 77]. MMD defined in Reproducing Kernel Hilbert Space (RKHS) is a squared distance between kernel embeddings of marginal distributions $P(X_s)$ and $Q(X_t)$. The formula of

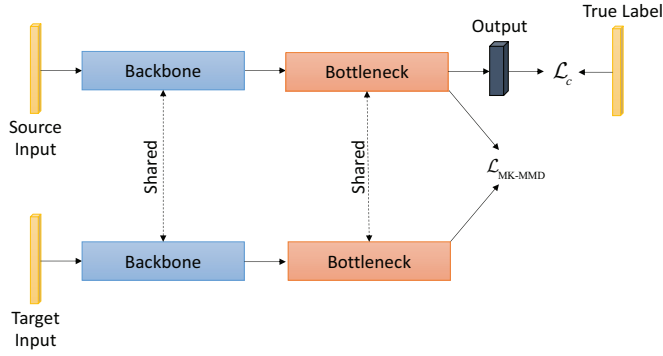


Fig. 3. The UDTL-based model based on MK-MMD.

MMD is written as follows:

$$\mathcal{L}_{\text{MMD}}(P, Q) = \left\| \mathbb{E}_P(\phi(x^s)) - \mathbb{E}_Q(\phi(x^t)) \right\|_{\mathcal{H}_k}^2 \quad (7)$$

where \mathcal{H}_k represents RKHS using the kernel k (in general, Gaussian kernel is used as the kernel), $\phi(\cdot)$ represents the mapping to RKHS, and \mathbb{E} represents the mathematical expectation.

For real application, the parameter selection of each kernel is crucial to the final performance of the mapping. To tackle this problem, MK-MMD which could maximize the two-sample test power and minimize the Type II error jointly was proposed by Gretton et al [41]. For MK-MMD, researchers often use the convex combination of m kernels $\{k_u\}$ to provide effective estimation of the mapping.

$$K \triangleq \left\{ k = \sum_{u=1}^m \beta_u k_u : \sum_{u=1}^m \beta_u = 1, \beta \geq 0, \forall u \right\} \quad (8)$$

where $\{\beta_u\}$ are weighted parameters of different kernels (In this paper, all $\{\beta_u\} = 1$).

Inspired by deep adaptation networks (DAN) proposed in [42], we design an UDTL-based model by adding MK-MMD into the loss function to realize features shift between source and target domains shown in Fig. 3. In addition, the final loss function is defined as follows:

$$\mathcal{L} = \mathcal{L}_c + \lambda_{\text{MK-MMD}} \mathcal{L}_{\text{MK-MMD}}(\mathcal{D}_s, \mathcal{D}_t) \quad (9)$$

where $\lambda_{\text{MK-MMD}}$ is the trade-off parameter in this total loss and $\mathcal{L}_{\text{MK-MMD}}$ means the multi-kernel version of MMD. Besides, following the setting of most published papers, we simply use the Gaussian kernel and the number of kernels is equal to five. The bandwidth of each kernel is set to be the median pairwise distances on training data according to the median heuristic [41].

3.5.2. JMMD

MMD and MK-MMD which are defined to solve the problem $P(X_s) \neq Q(X_t)$ cannot be used to tackle the domain shift generated by joint distributions of inputs and outputs (e.g. $P(X_s, Y_s) \neq Q(X_t, Y_t)$). Thus, JMMD proposed in [45] was designed to measure the distance of empirical joint distributions $P(X_s, Y_s)$ and $Q(X_t, Y_t)$ between source and target

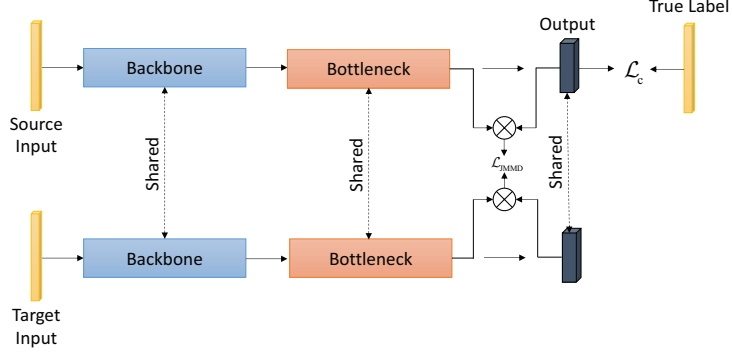


Fig. 4. The UDTL-based model based on JMMD.

domains. The formula of JMMD is written as follows [45]:

$$\mathcal{L}_{\text{JMMD}}(P, Q) = \left\| \mathbb{E}_P \left(\otimes_{l=1}^{|L|} \phi^l(z^{sl}) \right) - \mathbb{E}_Q \left(\otimes_{l=1}^{|L|} \phi^l(z^{tl}) \right) \right\|_{\otimes_{l=1}^{|L|} \mathcal{H}^l}^2 \quad (10)$$

where $\otimes_{l=1}^{|L|} \phi^l(x^l) = \phi^1(x^1) \otimes \dots \otimes \phi^{|L|}(x^{|L|})$ is the feature mapping in the tensor product Hilbert space, L is the set of higher network layers, $|L|$ is the number of layers in the corresponding set, z^{sl} means the activations of the l -th layer generated by the source domain, and z^{tl} means the activation of the l -th layer generated by the target domain.

Inspired by Joint Adaptation Network (JAN) which used JMMD to align the domain shift [45], we design an UDTL-based model by adding JMMD into the loss function to realize the features shift between the source and target domains shown in Fig. 4. The final loss function is defined as follows:

$$\mathcal{L} = \mathcal{L}_c + \lambda_{\text{JMMD}} \mathcal{L}_{\text{JMMD}}(\mathcal{D}_s, \mathcal{D}_t) \quad (11)$$

where λ_{JMMD} is the trade-off parameter in this total loss. In addition, the parameter setting of JMMD is the same as that in JAN.

3.5.3. CORAL

The CORAL loss, which aims to align the second-order statistics of source and target distributions, was first proposed in [78] and was further used in UDTL [38]. First of all, following [78] and [38], we give the definition of the CORAL loss as

$$\mathcal{L}_{\text{CORAL}}(\mathcal{D}_s, \mathcal{D}_t) = \frac{1}{4d^2} \|C_s - C_t\|_F^2 \quad (12)$$

where $\|\cdot\|_F$ is the Frobenius norm and d is the dimension of each sample. C_s and C_t defined in Eq. 13 are covariance matrices in source and target domains, respectively.

$$\begin{aligned} C_s &= \frac{1}{n_s - 1} \left(X_s^T X_s - \frac{1}{n_s} (\mathbf{1}^T X_s)^T (\mathbf{1}^T X_s) \right) \\ C_t &= \frac{1}{n_t - 1} \left(X_t^T X_t - \frac{1}{n_t} (\mathbf{1}^T X_t)^T (\mathbf{1}^T X_t) \right) \end{aligned} \quad (13)$$

where $\mathbf{1}$ represents the column vector whose elements are all equal to one.

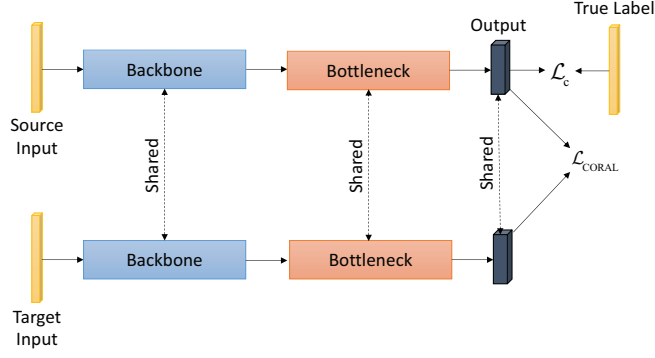


Fig. 5. The UDTL-based model based on CORAL.

Inspired by Deep CORAL proposed in [38], we design an UDTL-based model by adding the CORAL loss into the loss function to realize the feature transfer between source and target domains shown in Fig. 5. Also, the final loss function is defined as follows:

$$\mathcal{L} = \mathcal{L}_c + \lambda_{\text{CORAL}} \mathcal{L}_{\text{CORAL}}(\mathcal{D}_s, \mathcal{D}_t) \quad (14)$$

where λ_{CORAL} is the trade-off parameter of this total loss.

3.6. Adversarial-based DTL

Inspired by GAN, more and more researchers have embedded the idea of GAN in the field of DTL. Adversarial-based DTL refers to an adversarial method using a domain discriminator to reduce the feature distribution discrepancy between source and target data produced by a deep feature extractor. In this paper, we use two commonly used methods including domain adversarial neural network (DANN) [63] and conditional domain adversarial network (CDAN) [79] to represent adversarial-based methods and test corresponding accuracies.

3.6.1. DANN

Similar to MMD and MK-MMD, DANN is defined to solve the problem $P(X_s) \neq Q(X_t)$. It aims to train the feature extractor which is implemented to extract features from the input data, the domain discriminator which is implemented to distinguish source and target domains, and the class predictor which is implemented to predict the corresponding labels simultaneously to align source and target distributions ($P(X_s), Q(X_t)$). That is to say, DANN trains the feature extractor to make the domain discriminator difficult to distinguish differences between two domains. To explain DANN more clearly, we first define some symbols. G_f is the feature extractor whose parameters are θ_f , G_c is the class predictor whose parameters are θ_c , and G_d is the domain discriminator whose parameters are θ_d . After that, the prediction loss (the cross-entropy loss) and the adversarial loss (the binary cross-entropy loss) can be rewritten as follows

$$\mathcal{L}_c(\theta_f, \theta_c) = -\mathbb{E}_{(x_i^s, y_i^s) \in \mathcal{D}_s} \sum_{c=0}^{C-1} \mathbb{1}_{[y_i^s=c]} \log [G_c(G_f(x_i^s; \theta_f); \theta_c)] \quad (15)$$

$$\mathcal{L}_{\text{DANN}}(\theta_f, \theta_d) = -\mathbb{E}_{x_i^s \in \mathcal{D}_s} \log [G_d(G_f(x_i^s; \theta_f); \theta_d)] - \mathbb{E}_{x_i^t \in \mathcal{D}_t} \log [1 - G_d(G_f(x_i^t; \theta_f); \theta_d)] \quad (16)$$

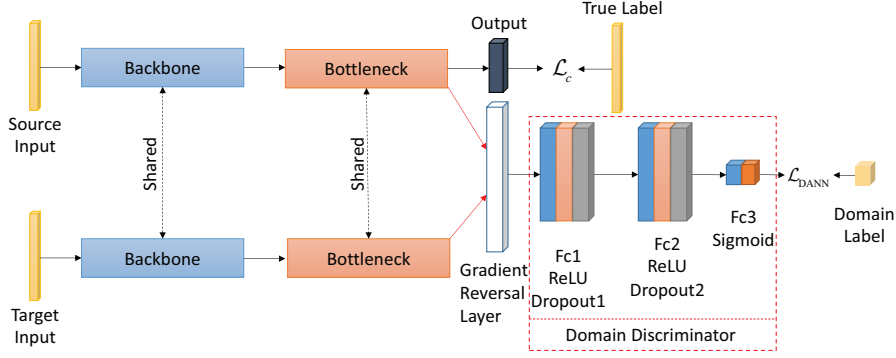


Fig. 6. The UDTL-based model based on DANN.

Table 3: Parameters of the domain discriminator.

Layers	Parameters
Fc1	out_features=2014
Dropout1	p=0.5
Fc2	out_features=1024
Dropout2	p=0.5
Fc3	out_features=2

To sum up, the total loss of DANN can be defined as

$$\mathcal{L}(\theta_f, \theta_c, \theta_d) = \mathcal{L}_c(\theta_f, \theta_c) - \lambda_{\text{DANN}} \mathcal{L}_{\text{DANN}}(\theta_f, \theta_d) \quad (17)$$

where λ_{DANN} is the trade-off parameter of this total loss.

During the training procedure, on one hand, we need to minimize the prediction loss to allow the feature extractor and the class predictor to predict the true label as much as possible. On the other hand, we also need to maximize the adversarial loss to make the domain discriminator difficult to distinguish differences between two domains. Thus, solving the saddle point $(\hat{\theta}_f, \hat{\theta}_c, \hat{\theta}_d)$ is equivalent to the following min-max optimization problem:

$$\begin{aligned} (\hat{\theta}_f, \hat{\theta}_c) &= \arg \min_{\theta_f, \theta_c} \mathcal{L}(\theta_f, \theta_c, \hat{\theta}_d) \\ (\hat{\theta}_d) &= \arg \max_{\theta_d} \mathcal{L}(\hat{\theta}_f, \hat{\theta}_c, \theta_d). \end{aligned} \quad (18)$$

Following the statement in [63], we can simply add a special *gradient reversal layer* (GRL), which changes signs of the gradient from the subsequent level and is parameter-free, to solve the above optimization problem.

We design an UDTL-based model by adding the adversarial idea into the loss function to realize the feature transfer between source and target domains shown in Fig. 6. As shown in Fig. 6, It can be observed that we use a three-layer fully-connected binary classifier as our domain discriminator which is the same as [63], and the parameters of these fully-connected layers are listed in Table 3.

3.6.2. CDAN

Though DANN can align the distributions of source and target domains efficiently, it may still exist some other bottlenecks. As stated in [79], DANN cannot capture complex multimodal structures and it is hard to condition the domain discriminator safely. Based on this statement, Long et al. [79] proposed a new adversarial-based DTL model

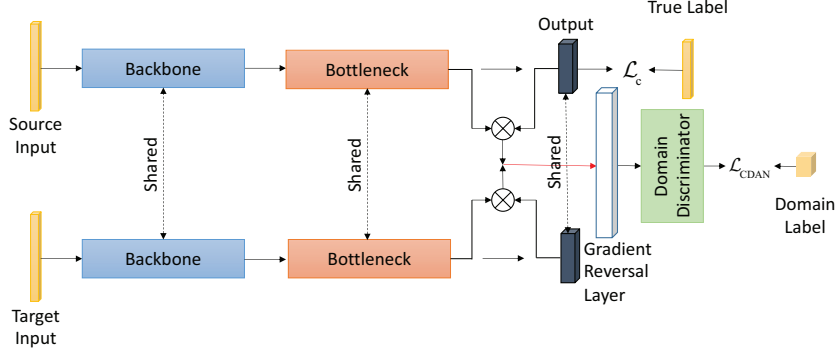


Fig. 7. The UDTL-based model based on CDAN.

called CDAN to solve the problem $P(X_s, Y_s) \neq Q(X_t, Y_t)$. To briefly introduce the main idea inside CDAN, we first need to define the multilinear map \otimes which means the outer product of multiple random vectors. If two random vectors x and y are given, the mean mapping $x \otimes y$ can capture complex multimodal structures inside the data completely. Besides, the cross-covariance $\mathbb{E}_{xy}[\phi(x) \otimes \phi(y)]$ can be used to model the joint distribution $P(x, y)$ successfully. Thus, the conditional adversarial loss is defined as follow

$$\mathcal{L}_{\text{CDAN}}(\theta_f, \theta_d) = -\mathbb{E}_{x_i^s \in \mathcal{D}_s} \log \left[G_d \left(G_f(x_i^s) \otimes G_c \left(G_f(x_i^s) \right) \right) \right] - \mathbb{E}_{x_i^t \in \mathcal{D}_t} \log \left[1 - G_d \left(G_f(x_i^t) \otimes G_c \left(G_f(x_i^t) \right) \right) \right], \quad (19)$$

and the prediction loss is the same as that in Eq. 15.

To relax the influence of samples with uncertain predictions, the entropy criterion $H(p) = -\sum_{c=0}^{C-1} p_c \log p_c$ is used to define the uncertainty of predictions by classifiers, where p_c is the probability of the predicting result corresponding to the label c . According to the defined entropy-aware weight function shown in Eq. 20, those hard-to-transfer samples are reweighted with lower weights in the modified conditional adversarial loss (21).

$$w(H(p)) = 1 + e^{-H(p)} \quad (20)$$

$$\begin{aligned} \mathcal{L}_{\text{CDAN}}(\theta_f, \theta_d) = & -\mathbb{E}_{x_i^s \in \mathcal{D}_s} w(H(p_i^s)) \log \left[G_d \left(G_f(x_i^s) \otimes G_c \left(G_f(x_i^s) \right) \right) \right] \\ & - \mathbb{E}_{x_i^t \in \mathcal{D}_t} w(H(p_i^t)) \log \left[1 - G_d \left(G_f(x_i^t) \otimes G_c \left(G_f(x_i^t) \right) \right) \right]. \end{aligned} \quad (21)$$

We design an UDTL-based model by embedding the conditional adversarial idea into the loss function to realize the feature transfer between source and target domains shown in Fig. 7. Also, the final loss function is defined as follows:

$$\mathcal{L}(\theta_f, \theta_c, \theta_d) = \mathcal{L}_c(\theta_f, \theta_c) - \lambda_{\text{CDAN}} \mathcal{L}_{\text{CDAN}}(\theta_f, \theta_d) \quad (22)$$

where λ_{CDAN} is the trade-off parameter of this total loss.

4. Applications of UDTL-based Intelligent Fault Diagnosis

The critical point of intelligent diagnosis is to recognize fault components including gears, bearings, rotors, etc. through different sources of data, such as vibration, current, and sound signals. In traditional intelligent diagnosis, training and testing samples are often split from the same experiment, which supposes that all the samples are from the same

domain. However, distributions of training and testing samples are often different, due to the influence of working conditions, fault sizes, fault types, etc. Consequently, UDTL-based intelligent diagnosis has been introduced recently to tackle this domain shift problem since there are some shared characteristics in the feature space. Using these shared characteristics, applications of UDTL-based intelligent diagnosis can be mainly classified into four categories: different working conditions, different types of faults, different locations, and different machines.

Different working conditions: In real industry applications, due to the influence of speed, load, temperature, etc. working conditions often vary with the operating time. Collected signals may contain the domain shift which means that the distributions of data may differ significantly under different work conditions [60]. The aim of UDTL-based intelligent diagnosis is that the model trained using collected signals under one operating condition is shifted to test on other signals under another different working condition. It also means that the trained model can adapt to different working conditions.

Different types of faults: In real industry applications, label differences between source and target domains may exist since different types of faults would happen on the same components. Therefore, there are three cases in the transfer learning problem. The first one is that unknown fault types appear in the target domain. The second one is that partial fault types of the source domain appear in the target domain. The third one is that the first two cases occur at the same time. The aim of UDTL-based intelligent diagnosis is that the model trained with some types of faults is shifted to test on the target domain with different types of faults.

Different locations: In real industry applications, because sensors installed on the same machine are often responsible for monitoring different key components, and sensors located near the fault are more suitable for indicating the fault information than those located far from the fault. However, key components in the same machine have different probability of failure rate, which leads to the situation where collected signals by different locations have different numbers of labeled data. The aim of UDTL-based intelligent diagnosis is that the model trained with plenty of labeled data from one location is shifted to test on the target domain with a lack of labeled data from other locations.

Different machines: In real industry applications, enough labeled fault samples of actual operating machinery are difficult to obtain because of the testing cost and security. Besides, enough labeled data can be generated from laboratory machines or computer simulations. However, distributions of data from laboratory machines or computer simulations are different but similar to distributions of data from actual operating machinery due to the similar structure of machines and similar measurement conditions. Thus, the aim of UDTL-based intelligent diagnosis is that the model trained using data from laboratory machines or computer simulations is shifted to test on data gathered from actual operating machinery.

5. Datasets

In the field of intelligent fault diagnosis, open source datasets are very important for development, comparison and evaluation of different models. In this comparative study, we mainly test five datasets to verify the performance of different transfer learning strategies mentioned above. The detailed description of five datasets is given as follows:

5.1. Case Western Reserve University (CWRU) dataset

The CWRU dataset provided by Case Western Reserve University Bearing Data Center [80] is one of the most famous open source datasets in the fault diagnosis research and is used by a large number of published papers including DTL in intelligent fault classification. Data of CWRU was collected by accelerometers attached to the housing with magnetic

Table 4: The description of class labels of CWRU.

Class Label	0	1	2	3	4	5	6	7	8	9
Fault Location	NA	IF	BF	OF	IF	BF	OF	IF	BF	OF
Fault Size (mils)	0	7	7	7	14	14	14	21	21	21

Table 5: The transfer learning tasks of CWRU.

Task	0	1	2	3
Load (HP)	0	1	2	3
Speed (rpm)	1797	1772	1750	1730

Table 6: The transfer learning tasks and operating parameters of PU.

Task	0	1	2	3
Load Torque (Nm)	0.7	0.7	0.1	0.7
Radial Force (N)	1000	1000	1000	400
Speed (rpm)	1500	900	1500	1500

bases. Following most of published papers, this paper also uses the drive end bearing fault data whose sampling frequency is equal to 12 kHz and ten bearing conditions are listed in Table 4. In Table 4, one normal bearing (NA) and three fault locations including inner fault (IF), ball fault (BF) and outer fault (OF) are classified into ten categories (one health state and nine fault states) according to different fault sizes.

Besides, as shown in Table 5, the CWRU dataset consists of four different motor loads that correspond to four different operating speeds. For the transfer learning task, this paper considers these different working conditions as different tasks including 0, 1, 2, and 3. For example, Task 0 \rightarrow 1 means that the source domain is data with a motor load equal to 0 HP and the target domain is data with a motor load equal to 1 HP. In total, there are 12 transfer learning setups in this dataset.

5.2. Paderborn University (PU) dataset

The PU dataset acquired from Paderborn University is a 6203 bearing dataset [81, 82] which consists of artificially induced and real damages. Vibration signals of the bearing housing were collected by a piezoelectric accelerometer with the sampling frequency equal to 64 kHz. By changing the rotational speed of the drive system, the radial force onto the test bearing, and the load torque on the drive train, the PU dataset consists of four operating conditions as shown in Table 6.

On the one hand, thirteen bearings with real damages caused by accelerated lifetime tests [81] are used to study the transfer learning tasks among different working conditions (twenty experiments were performed on every bearing code, and every experiment sustained 4 seconds. In this paper, we only choose the former one experiments to test the methods). The categorization information of bearings with real damages is presented in Table 7 (the meaning of contents in the table is explained in [81]). For transfer tasks, Task 0 \rightarrow 1 means that the source domain is data with rotational speed equal to 1500 rpm, load torque equal to 0.7 Nm, and radial force equal to 1000 N, and the target domain is data with rotational speed equal to 900 rpm, load torque equal to 0.7 Nm, and radial force equal to 1000 N. In total, there are twelve transfer learning setups in this dataset.

5.3. JiangNan University (JNU) dataset

The JNU dataset is a bearing dataset acquired by Jiang Nan University, China. (this dataset can be downloaded from [83] and researchers can refer to [84] for more detailed information.) Four kinds of health conditions, including

Table 7: The information of bearings with real damages.

Bearing Code	Damage	Bearing Element	Combination	Characteristic of Damage	Label
KA04	fatigue: pitting	OR	S	single point	0
KA15	plastic deform: indentations	OR	S	single point	1
KA16	fatigue: pitting	OR	R	single point	2
KA22	fatigue: pitting	OR	S	single point	3
KA30	plastic deform: indentations	OR	R	distributed	4
KB23	fatigue: pitting	IR(+OR)	M	single point	5
KB24	fatigue: pitting	IR(+OR)	M	distributed	6
KB27	plastic deform: indentations	OR+IR	M	distributed	7
KI14	fatigue: pitting	IR	M	single point	8
KI16	fatigue: pitting	IR	S	single point	9
KI17	fatigue: pitting	IR	R	single point	10
KI18	fatigue: pitting	IR	S	single point	11
KI21	fatigue: pitting	IR	S	single point	12

OR: outer ring; IR: inner ring;
S: single damage; R: repetitive damage; M: multiple damages

Table 8: The label information of JNU.

Fault mode	Label
Inner ring	0
Normal state	1
Outer ring	2
Rolling element	3

Table 9: The transfer learning tasks of JNU.

Task	0	1	2
Speed (rpm)	600	800	1000

normal state, inner ring fault, outer ring fault, and roller element fault, were carried out in the experiment shown in Table 8. Vibration signals were sampled under three different rotation speeds (600 rpm, 800 rpm, and 1000 rpm) using accelerometers with the sampling frequency of 50 kHz. As shown in Table 9, different working conditions are considered as different transfer learning tasks. For instance, Task 0 \rightarrow 1 means that the source domain is data with rotation speed equal to 600 rpm and the target domain is data with rotation speed equal to 800 rpm.

5.4. PHM Data Challenge on 2009 (PHM) dataset

The PHM dataset is generic industrial gearbox data provided by the PHM Data Challenge competition [85]. The industrial gearbox consists of three shafts (input shaft, idler shaft, and output shaft), six bearings and four gears (including two spur gears and two helical gears). The dataset was collected by two accelerometers and one tachometer mounted on the input shaft (for collecting rotating speed), the input shaft retaining plate, and the output shaft retaining plate, respectively. The sampling frequency is set to 200 KHz/3. Fourteen experiments (eight for spur gears and six for helical gears) were performed.

In this paper, we utilize helical gears dataset (six conditions) sampled from accelerometers mounted on input shaft retaining plates. The dataset contains five different rotating speeds and two different loads, and thus, there are 12 tasks in this dataset. However, in order to save the computational time, data collected from the former four shaft speeds under the high load are considered as presented in Table 10. For transfer learning tasks, Task 0 \rightarrow 1 means that the source domain is data with shaft speed equal to 30 Hz and the target domain is data with shaft speed equal to 35 Hz. In total, there are

Table 10: The transfer learning tasks of PHM.

Task	0	1	2	3
Speed (Hz)	30	35	40	45
Load	High	High	High	High

Table 11: The transfer learning tasks of SEU.

Class Label	Location	Type	Description
0	Gear	Health	
	Bearing		
1	Bearing	Ball	Crack occurs in the ball
2	Bearing	Outer	Crack occurs in the outer ring
3	Bearing	Inner	Crack occurs in the inner ring
4	Bearing	Combination	Crack occurs in the inner ring and outer ring
5	Gear	Chipped	Crack occurs in the gear feet
6	Gear	Miss	Missing one of the feet in the gear
7	Gear	Surface	Wear occurs in the surface of the gear
8	Gear	Root	Crack occurs in the root of the gear feet

twelve transfer learning setups in this dataset.

5.5. Southeast University (SEU) dataset

The Southeast University (SEU) dataset is a gearbox dataset provided by Southeast University, China [20, 86]. This dataset consists of two sub-datasets, including the bearing dataset and the gear dataset, which were both collected from Drivetrain Dynamics Simulator. During the experiment, eight channels are collected, and in this paper, we use the data from the channel 2. As shown in Table 11, each sub-dataset consists of five conditions: one health state and four fault states. So there are nine conditions in total.

Two kinds of working conditions with rotating speed - load configuration set to be 20 HZ - 0 V and 30 HZ - 2 V are considered as different tasks including 0 and 1. For example, Task 0 \rightarrow 1 means that the source domain is data with 20 Hz rotating speed and 0 V load and the target domain is data with 30 Hz rotating speed and 2 V load. In total, there are two transfer learning setups in this dataset.

6. Data Preprocessing and Splitting

Data preprocessing and splitting are two important aspects in terms of performance of UDTL-based intelligent fault diagnosis. Although UDTL-based methods often have automatic feature learning capabilities (also called end-to-end learning), sometimes, some data processing steps can help UDTL-based models to achieve better performance, such as Short-time Fourier Transform (STFT) in speech signal classification and the data normalization in the image recognition. Besides, there often exist some pitfalls in the training process, mainly including test leakage. That is to say, testing samples are used in the training process.

6.1. Input Types

There are two kinds of input types testing in this paper including the time domain input and the frequency domain input. For the time domain input, measured vibration signals are used as the input of models directly and the length of each sample is 1024 without any overlapping. For the frequency domain input, measured vibration signals are first

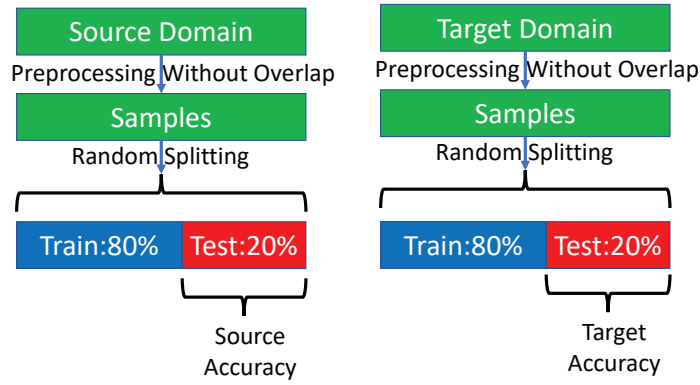


Fig. 8. Data splitting for UDTL-based intelligent diagnosis methods.

transformed into the frequency domain through Fast Fourier Transform (FFT) and the length of each sample is 512 due to the symmetry of spectral coefficients.

6.2. Normalization

Data normalization is often the basic procedure in UDTL-based intelligent fault diagnosis, which can keep the input values into a certain range. In this paper, we use the Z-score normalization which is formulated as follows:

$$x_i^{normalize} = \frac{x_i - x_i^{mean}}{x_i^{std}}, \quad i = 1, 2, \dots, N \quad (23)$$

where x_i is the input data, x_i^{mean} is the mean value of x_i , and x_i^{std} is the standard deviation of x_i .

6.3. Data Splitting

There often exist some pitfalls in data splitting, mainly including test leakage. First of all, since this paper does not use the validation set to select the best model, the splitting of the validation set is ignored here. In UDTL-based intelligent fault diagnosis, datasets in the target domain are also used in the training procedure to realize the migration of models between two domains. Meanwhile, for UDTL-based methods which are mainly discussed in this paper, datasets in the target domain are also used as the testing sets. In fact, datasets in these two conditions should not overlap, otherwise there would exist test leakage. Therefore, as shown in Fig. 8, we take 80% of total samples as the training set and 20% of total samples as the test set in source and target domains respectively to avoid this test leakage.

7. Evaluation Methodology

7.1. Evaluation Metrics

The overall accuracy and the average accuracy are often used to evaluate the performance of UDTL-based intelligent fault diagnosis. To keep things simple and comprehensible, we use the overall accuracy which is defined as the number of correctly classified samples divided by the total number of samples in testing datasets to verify the performance of different models. To avoid the randomness, we perform the experiments five times, and mean and maximum values of the overall accuracy are used to evaluate the final performance due to the fact that the variance of accuracies of five experiments is not statistically useful. In this paper, to save the test time, we use mean and maximum accuracies in the last epoch denoted as Last-Mean and Last-Max to represent the testing accuracies without any test leakage. Meanwhile,

we also list mean and maximum accuracies denoted as Best-Mean and Best-Max in the epoch where models achieve the best performance (it should be noted that these accuracies are dangerous due to the usage of testing set to choose the best model, which is one kind of test leakage).

7.2. Experimental Setting

We implement all UDTL-based intelligent fault diagnosis models discussed in this paper in **Pytorch** and put them into a unified code framework to make the testing process more reasonable. Each model is trained for 300 epochs, and during the training procedure, model training and testing processes are alternated. It should also be noted that for MK-MMD, JMMD, CORAL, DANN, and CDAN, we train models with source samples in the former 50 epochs to get a so-called pretrained model, and then transfer learning strategies are activated. We adapt mini-batch Adam to do the back-propagation during the training process and the batchsize is equal to 64. The “step” strategy in **Pytorch** is used as the learning rate annealing method, and the initial learning rate is 0.001 with a decay (multiplied by 0.1) in the epoch 150 and 250, respectively. For AdaBN, we update the statistics of BN layers through each batch for 3 extra epochs. For MK-MMD, JMMD, CORAL, DANN, and CDAN, we use a progressive training method increasing the trade-off parameter from 0 to 1 by multiplying to $\frac{1 - \exp(-\gamma e)}{1 + \exp(-\gamma e)}$ [79], where $\gamma = 10$ and e means the training progress changing from 0 to 1 after the transfer learning strategies are activated. In addition, all experiments are executed under Window 10 and **Pytorch 1.3** running on a computer with an Intel Core i7-9700K, GeForce RTX 2080Ti, and 16G RAM.

8. Evaluation Results

We will discuss evaluation results of five datasets, and final accuracies are shown in **Appendix A** (the maximum value of each row is bolded). To make the accuracies more readable, we use some visualization methods to present the results.

8.1. Results of Datasets

To make comparisons clearer, we summarize the overall best accuracies of different datasets among all methods, and results are shown in Fig. 9. It can be noted that CWRU and JNU can achieve accuracy over 95% and other datasets can only achieve an accuracy of around 60%. It is also worth mentioning that these accuracies are just a lower bound due to the fact that it is very hard to fine-tune every parameter in detail resulting from the uncertainty of UDTL-based intelligent fault diagnosis which we can see in following discussions.

8.2. Results of Models

Results of different methods under different datasets are shown in Fig. 10 to Fig. 14, and Fig. 14 is not set as the radar chart because two transfer tasks are not suitable for this visualization. For all datasets, all UDTL-based methods discussed in this paper can improve the accuracy of Basis (directly use the trained model in the source domain to test the unlabeled data in the target domain), except CORAL. For CORAL, it can only improve the accuracy in CWRU with the frequency domain input or in some single transfer tasks. For AdaBN, the improvement is much smaller than other methods.

In general, results of JMMD are better than those of MK-MMD, which indicates that the assumption of joint distributions in source and target domains is useful for improving the performance. Results of DANN and CDAN are generally better than those of MK-MMD, which indicates that the domain adversarial training is helpful for aligning the domain shift.

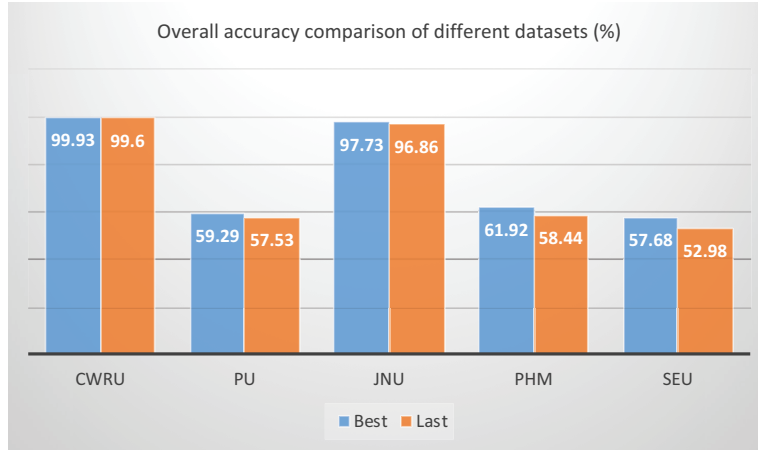


Fig. 9. The best accuracies of different datasets among all methods.

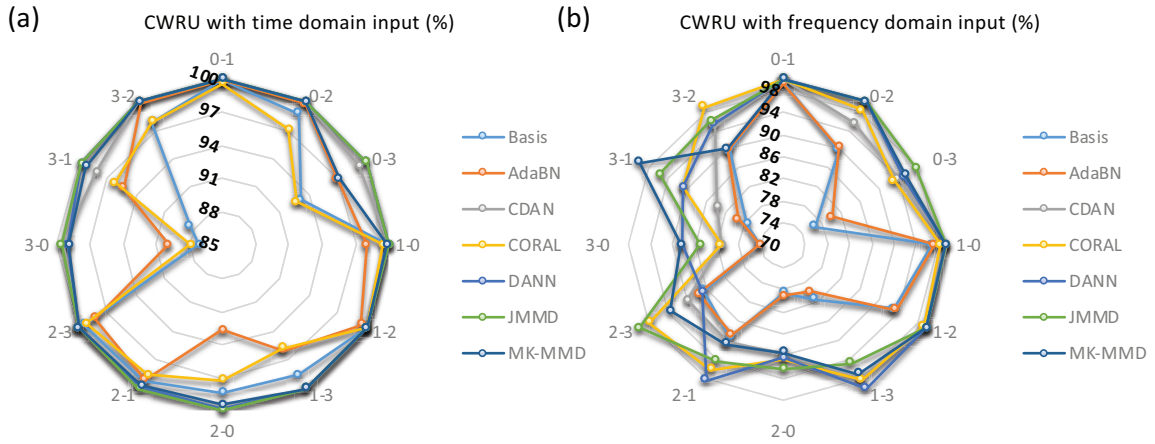


Fig. 10. The accuracy comparison of different methods in CWRU.

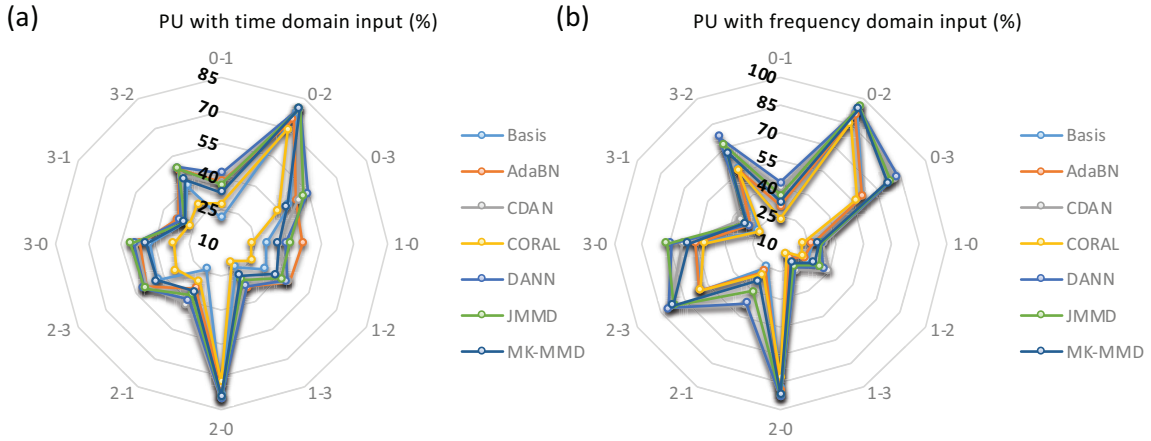


Fig. 11. The accuracy comparison of different methods in PU.

8.3. Results of Input Types

Accuracy comparisons of two input types with different datasets are shown in Fig. 15, and it can be concluded that the time domain input achieves better accuracies in CWRU, JNU, and SEU, while the frequency domain input gets better accuracies in PU and PHM. Besides, the accuracy gap between these two input types is relatively large, and we cannot simply infer which one is better due to the influence of backbones.

Thus, for a new dataset, we should test results of different input types instead of just using the more advanced tech-

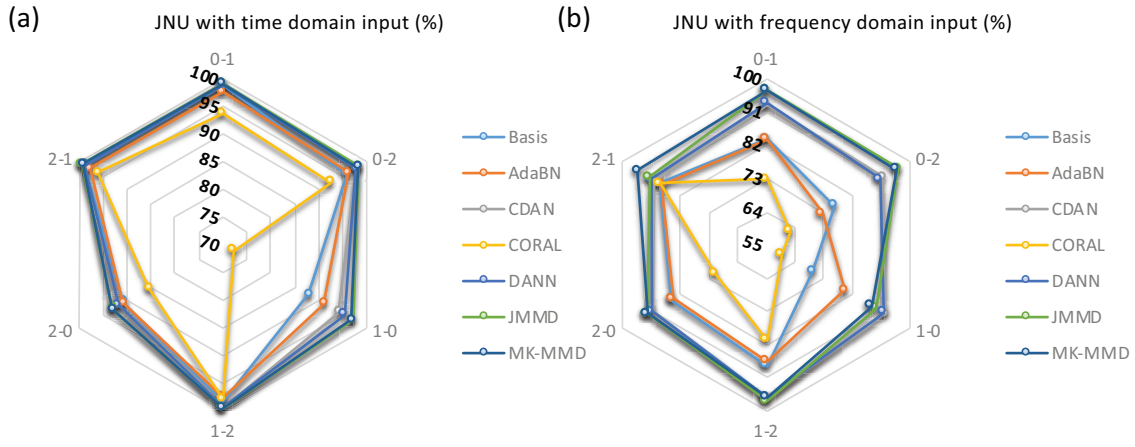


Fig. 12. The accuracy comparison of different methods in JNU.

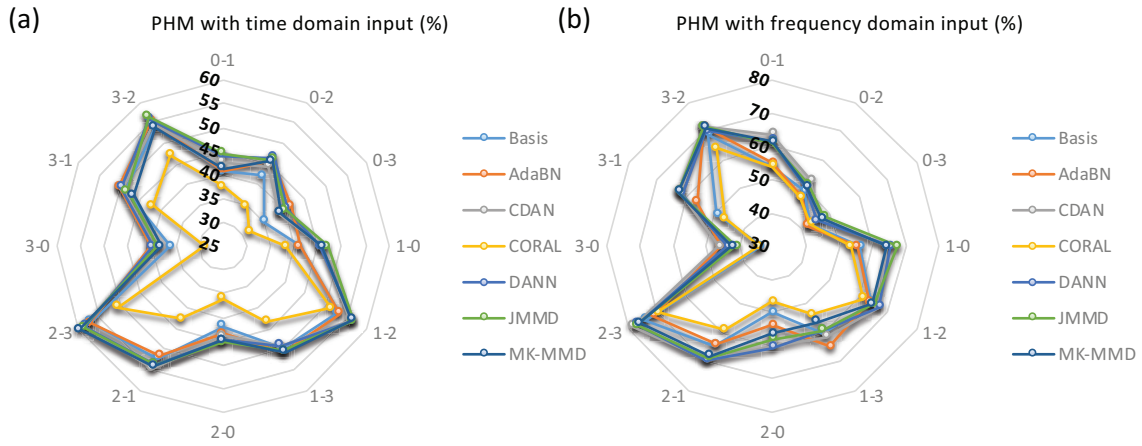


Fig. 13. The accuracy comparison of different methods in PHM.

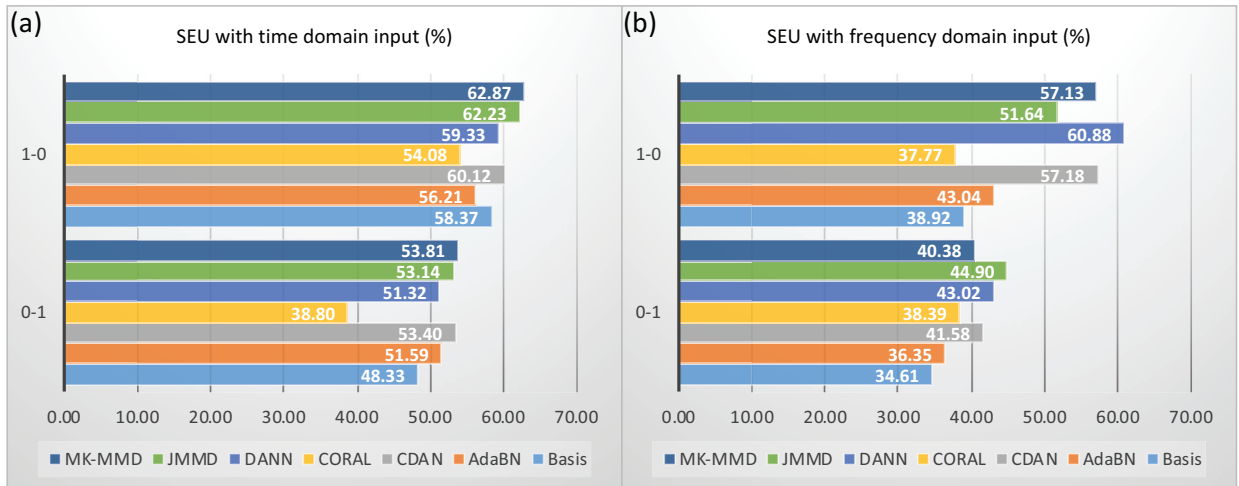


Fig. 14. The accuracy comparison of different methods in SEU.

niques to improve the performance of one input type due to the fact that using a different input type may improve the accuracy more efficient than using advanced techniques.

8.4. Results of Accuracy Types

As mentioned in Section 7, we use four kinds of accuracies including Best-Mean, Best-Max, Last-Mean, and Last-Max to represent the testing accuracies. As shown in Fig. 16, the fluctuation of different experiments is sometimes large,

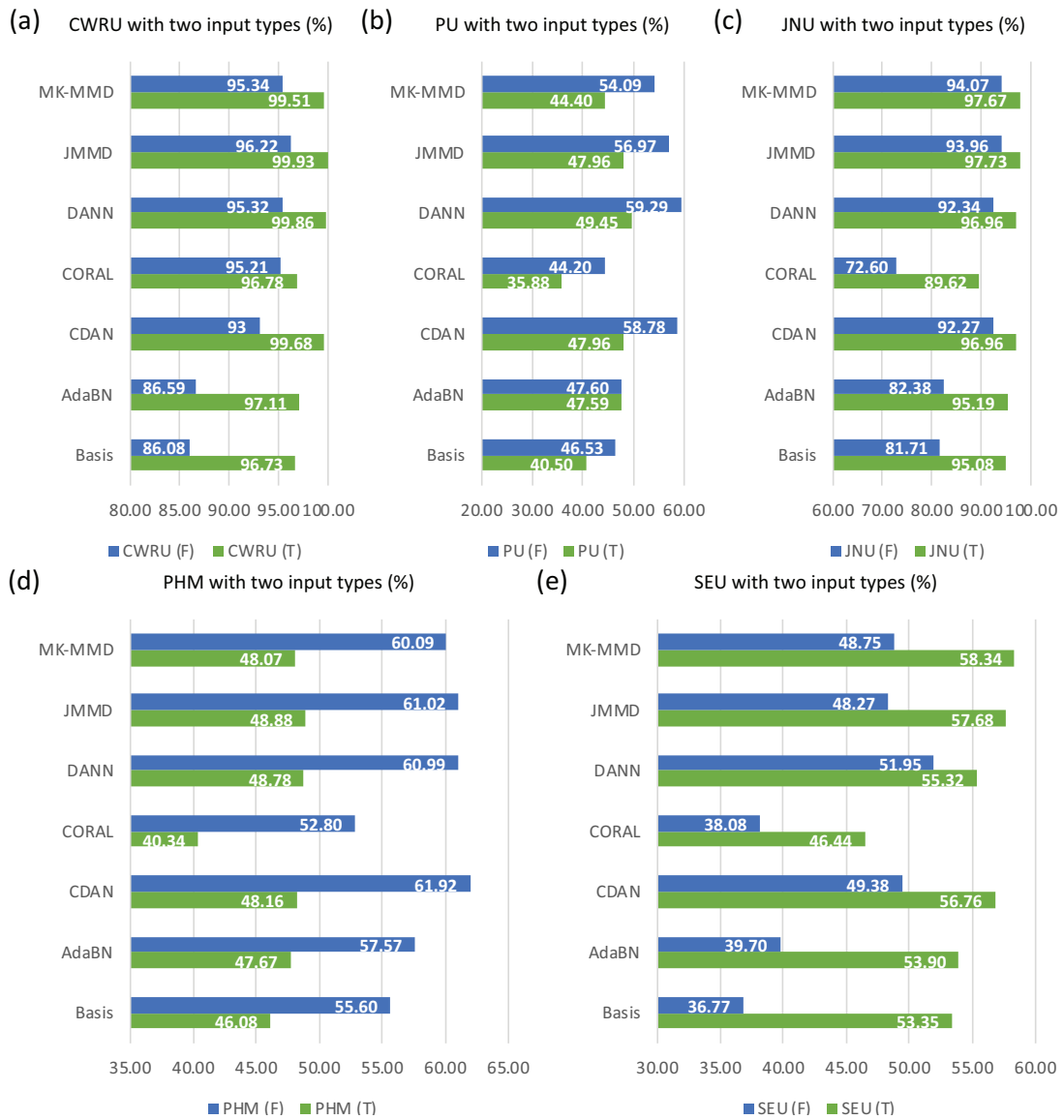


Fig. 15. The accuracy comparisons of two input types with different datasets. (F) means the frequency domain input, and (T) means the time domain input.

especially for those datasets whose overall accuracies are not very high, which indicates that the used algorithms are not very stable and robust. Besides, it seems that the fluctuation of the time domain input is smaller than that of the frequency domain input, and the reason may be that the backbone used in this paper is more suitable for the time domain input.

As shown in Fig. 17, the fluctuation of different experiments is also large, which is dangerous for testing the true performance of methods. Since Best uses the testing set to choose the best model (it is a kind of test leakage), Last may be more suitable for representing the generalization accuracy.

Thus, on one hand, the stability and robustness of UDTL-based algorithms need more attention instead of just improving accuracies. On the other hand, as we analyze above, accuracies of the last epoch (Last) are more suitable for representing the generalization ability of algorithms when the fluctuation between Best and Last is large.

It should also be mentioned that results shown in Fig. 16 and Fig. 17 are the overall differences, while, some transfer tasks which are named as easy tasks in every dataset can have small differences.

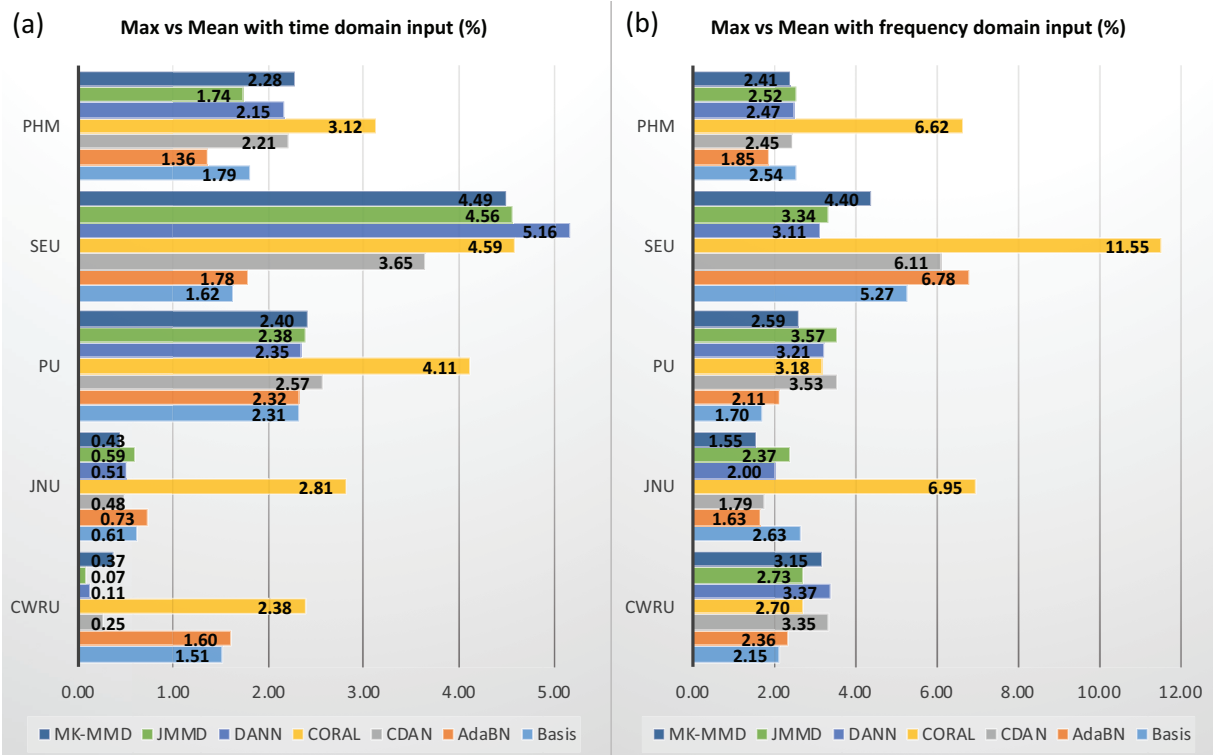


Fig. 16. The difference between Max and Mean according to Best average.

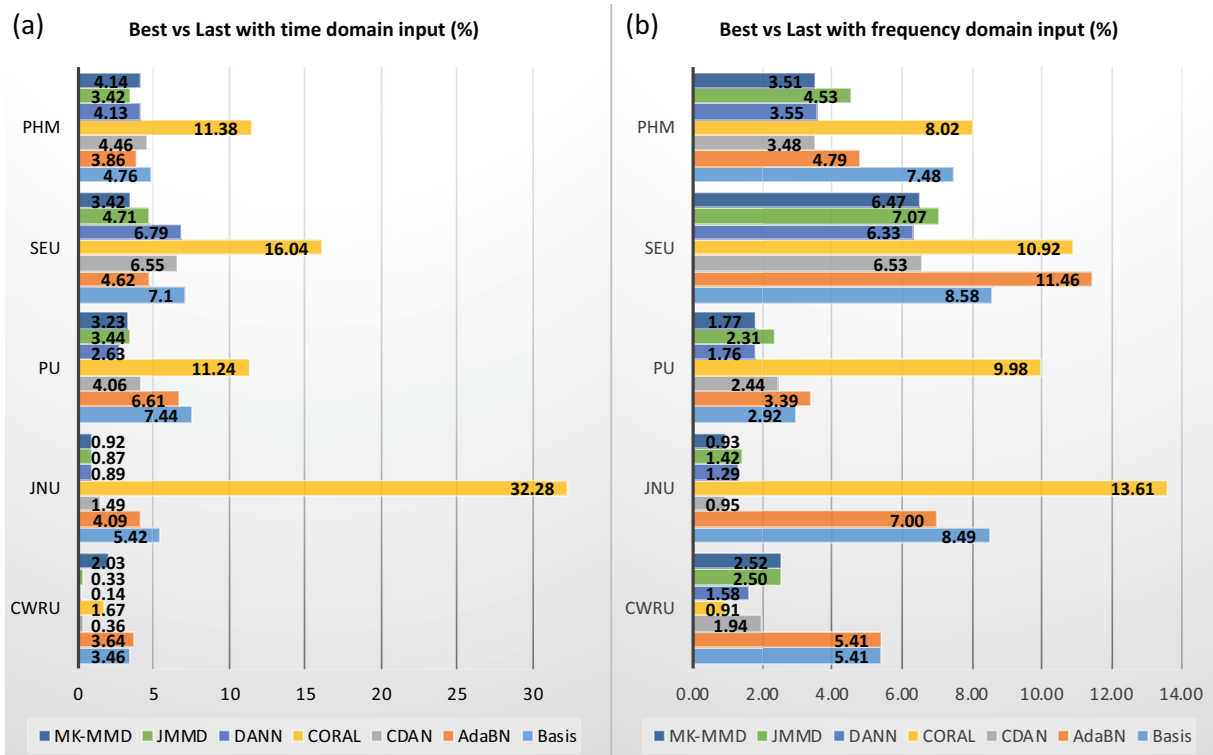


Fig. 17. The difference between Best average and Last average according to Mean.

9. Further Discussions

9.1. Transferability of Features

The reason why DL models embedded transfer learning methods can achieve breakthrough results in computer vision, especially for some domain adaptation datasets such as Office-31 and Caltech-10, is that many studies have shown and

proved that DL models can learn more transferable features for these tasks than traditional hand-crafted features [87, 88]. Meanwhile, features learned in the former layers are interpretable (for example, features learned by the first layer of each DL model resemble either Gabor filters or color blobs by training on the image dataset). In spite of the ability to learn general and transferable features, DL models also exist transition from general features to specific features and its transferability drops significantly in the last layers [88]. Therefore, fine-tuning DL models or adding various transfer learning strategies into the training process need to be investigated for realizing the valid transfer.

However, in the field of intelligent fault diagnosis, there is no research about how transferable are features in DL models, and actually, answering this problem is the most important cornerstone in DTL-based intelligent fault diagnosis. Since the aim of this paper is to give a comparative accuracy and release a code library, we just assume that the bottleneck layer is the task-specific layer and its output features are restrained with various transfer learning strategies (therefore, the final accuracy is not very high). Thus, it is imperative and vital for researchers to study the transferability of features and answer the question about how transferable features are learned from DL models. It should also be noted that in order to understand transferability of features more reasonable, we suggest that researchers may need to visualize the neurons to analyze the learned features by existing visualization algorithms, like [89, 90].

9.2. Influence of Backbones

In the field of domain adaptation for computer vision, many strong CNN models (also called backbones), such as AlexNet [2], VGG [72], GoogleNet [73], and ResNet [74] can be extended without caring about the model selection, which allows designing DTL-based algorithms more comparable and reasonable. Researchers often use the same backbones to test the performance of the proposed algorithms and can pay more attention to construct specific algorithms to align source and target domains.

However, in the field of intelligent fault diagnosis, the backbones of published DTL-based algorithms are often different, which makes the results hard to compare directly, and the influence of different backbones has never been studied thoroughly. Whereas, backbones of DTL-based algorithms do have a huge impact on results from comparisons between CWRU with the frequency domain input and “Table II” in [68] (the main difference is the architecture of backbones used in this paper and [68]). It can be observed that accuracies related to the task 3 in CWRU with the frequency domain input are much worse than those in “Table II” [68]. However, the backbone used in this paper can achieve excellent results shown in CWRU with the time domain input and some accuracies are even stronger than those in [68]. To make a stronger statement, we also use the well-known backbone in the field of computer vision called ResNet18 (it is also worth mentioning that we modify the structure of ResNet18 to adapt to one dimensional input) to test SEU and PHM datasets for explaining the huge impact of backbones. From comparisons of PHM shown in Fig. 18, ResNet18 can improve the accuracy of each transfer learning algorithm significantly. Besides, from comparisons of SEU shown in Fig. 19, ResNet18 with the time domain input actually reduces the accuracy, and on the contrary, ResNet18 with the frequency domain input improve the accuracy significantly. In summary, different backbones behave differently on different datasets with different input types.

Therefore, finding a strong and suitable backbone which can learn more transferable features for intelligent fault diagnosis according to different inputs is also very important for DTL-based algorithms (sometimes choosing a more effective backbone is even more important than using the more advanced transfer learning algorithms), and we suggest

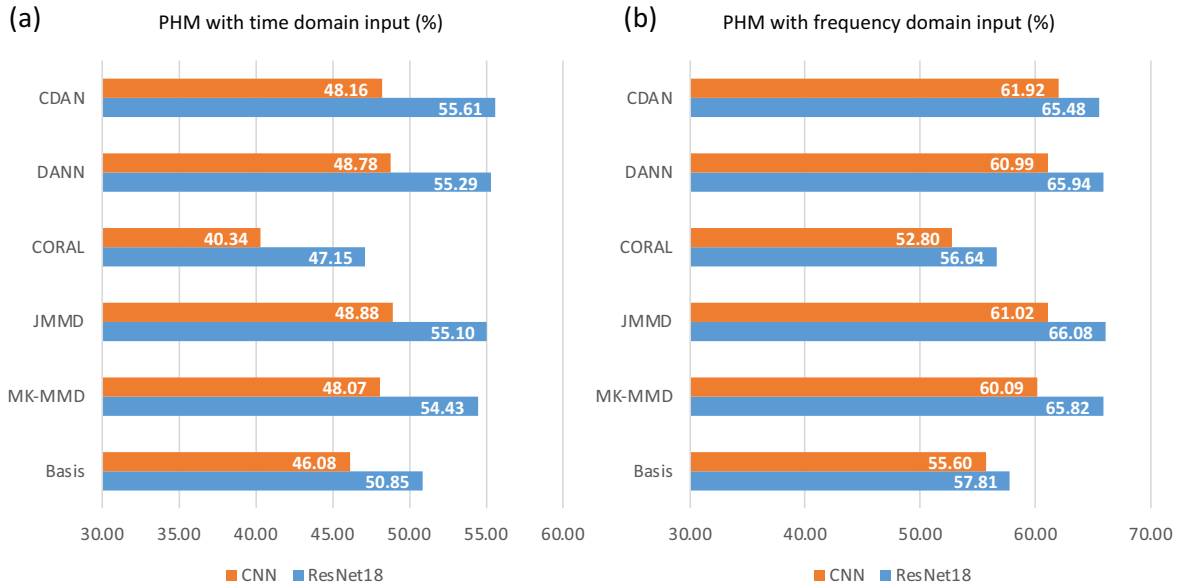


Fig. 18. Comparisons of PHM.

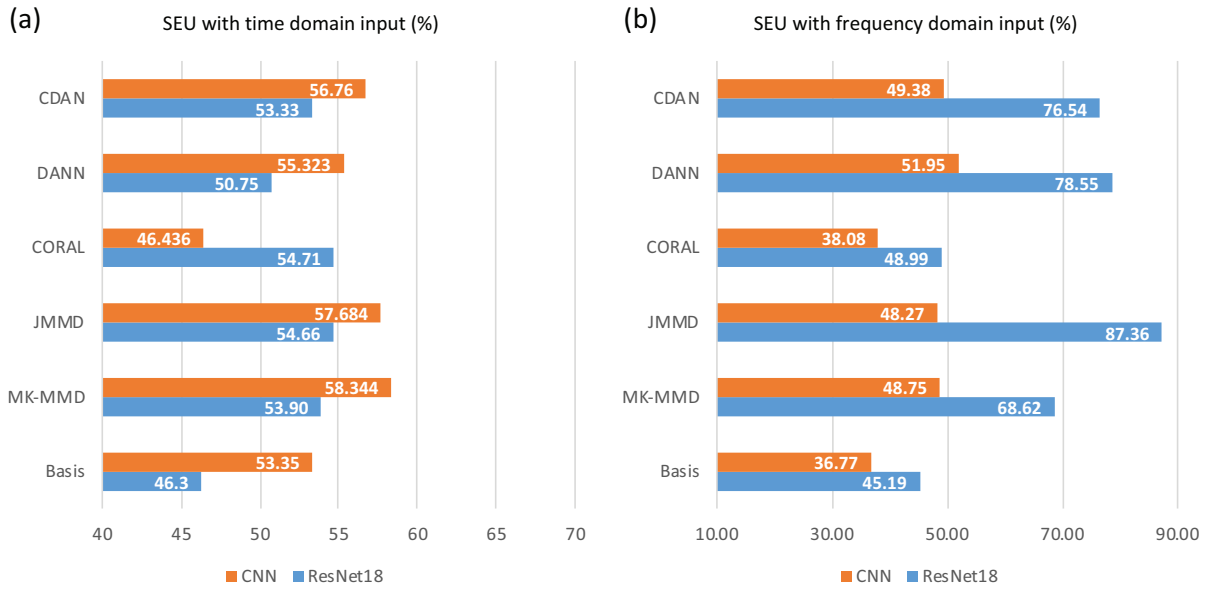


Fig. 19. Comparisons of SEU.

that researchers should first find a strong backbone and then use the same backbones to compare the results to avoid unfair comparisons.

9.3. Negative Transfer

As we discussed in Section 4, there are mainly four kinds of applications of UDTL-based intelligent fault diagnosis, and all experiments with five datasets are about transfer learning of different working conditions. To state that domain shifts of applications are not always suitable for generating the positive transfer, we use the PU dataset to design another transfer task considering the transfer between different methods of generating damages. The electric engraver is regarded as one of the methods. Due to insufficient labels of drilling and electrical discharge machining (EDM), we combine these two methods as one. Each method consists of three health conditions. Detailed information is listed in Table 12. For transfer tasks, Task 0 \rightarrow 1 means that the source domain is fault data generating through electric engraver and the target domain is fault data generating through EDM or drilling. There are two transfer learning setups in total.

Table 12: The information of bearings with artificial damage.

Task	Precast Method	Damage Location	Damage Extent	Bearing Code	Label
0	Electric Engraver	OR	1	KA05	0
	Electric Engraver	OR	2	KA03	1
	Electric Engraver	IR	1	KI03	2
1	EDM+Drilling	OR	1	KA01+KA07	0
	Drilling	OR	2	KA08	1
	EDM	IR	1	KI01	2

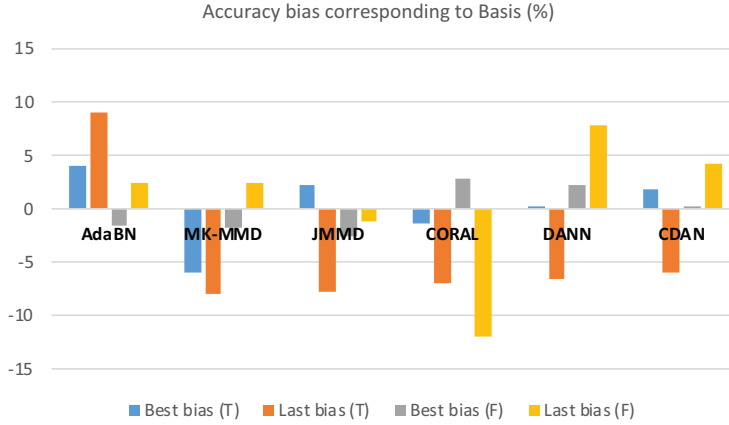


Fig. 20. The accuracy biases of these five methods corresponding to Basis. (F) means the frequency domain input, and (T) means the time domain input.

The transfer results are shown in Fig. 20 and **Appendix A** called PU-Types, it can be observed that each method has a negative transfer with the time or frequency domain inputs, and this phenomenon indicates that this constructed task may not be suitable for the transfer learning task. Actually, in the field of fault diagnosis, there are also some published papers designing transfer learning tasks which tackle transferring the gear samples to the bearing samples (it may not be a reliable transfer task) or transferring the experimental data to the real data (if the structures of two machines are different, it also may not be a reliable transfer task). Thus, it is very important to first figure out whether this question is suitable for transfer learning and whether two domains do have shared features.

9.4. Physical Priors

In the field of transfer learning for computer vision and natural language processing, new methods often use the existing knowledge or laws to provide a meaningful explanation, such as attention mechanism [91] and multimodal structures [79].

However, for UDTL-based fault diagnosis, many researchers only introduce methods which have already existed in the transfer learning field to perform fault diagnosis tasks and pay less attention to the prior knowledge behind the data (lack of using special phenomena or rules in fault diagnosis), which may cause the problem about overfitting the used datasets. Therefore, we suggest that scholars can learn from studies in the field of transfer learning (not just use the existing methods) and introduce prior knowledge of fault diagnosis into proposed transfer learning methods, to construct more targeted and suitable diagnostic models with higher recognition rates in industrial applications.

10. Conclusion

In this paper, we gather five publicly available datasets (CWRU, PU, JNU, PHM, and SEU) to perform a comparative analysis of four kinds UDTL-based intelligent fault diagnosis methods which include Basis, AdaBN, MK-MMD, JMMD,

CORAL, DANN, and CDAN from several perspectives. Based on the systematically comparative study, we conclude some useful results which might be helpful for further research. Firstly, the accuracies of CWRU and JNU are larger than 95%. Secondly, the results of different methods under different datasets indicate that the assumption of joint distributions and the domain adversarial training are two helpful techniques for promoting the accuracies. Thirdly, different input types often behave differently on each dataset, and choosing a suitable input type might also be important for improving the accuracies. Finally, the stability and robustness of UDTL-based intelligent fault diagnosis need to be taken seriously. To sum up, it might be useful for scholars to think ahead of these results before developing new models.

Also, we release the code library at <https://github.com/ZhaoZhibin/UDTL> and try to give a benchmark (it is worth mentioning that results are just a lower bound of the accuracy) performance of current algorithms to find the core that determines the transfer performance of algorithms to guide future research.

Acknowledgment

This work was supported by National Natural Science Foundation of China (No. 51835009, No. 51705398).

References

- [1] Y. LeCun, Y. Bengio, G. Hinton, Deep learning, *nature* 521 (2015) 436.
- [2] A. Krizhevsky, I. Sutskever, G. E. Hinton, Imagenet classification with deep convolutional neural networks, in: *Advances in neural information processing systems*, pp. 1097–1105.
- [3] G. E. Hinton, R. R. Salakhutdinov, Reducing the dimensionality of data with neural networks, *science* 313 (2006) 504–507.
- [4] A. Ng, et al., Sparse autoencoder, *CS294A Lecture notes* 72 (2011) 1–19.
- [5] S. J. Pan, Q. Yang, A survey on transfer learning, *IEEE Transactions on knowledge and data engineering* 22 (2009) 1345–1359.
- [6] K. Weiss, T. M. Khoshgoftaar, D. Wang, A survey of transfer learning, *Journal of Big data* 3 (2016) 9.
- [7] C. Tan, F. Sun, T. Kong, W. Zhang, C. Yang, C. Liu, A survey on deep transfer learning, in: *International Conference on Artificial Neural Networks*, Springer, pp. 270–279.
- [8] M. Wang, W. Deng, Deep visual domain adaptation: A survey, *Neurocomputing* 312 (2018) 135–153.
- [9] J. Xie, L. Zhang, L. Duan, J. Wang, On cross-domain feature fusion in gearbox fault diagnosis under various operating conditions based on transfer component analysis, in: *2016 IEEE international conference on prognostics and health management (ICPHM)*, IEEE, pp. 1–6.
- [10] A. Zhang, X. Gao, Supervised dictionary-based transfer subspace learning and applications for fault diagnosis of sucker rod pumping systems, *Neurocomputing* 338 (2019) 293–306.
- [11] H. Zheng, R. Wang, Y. Yang, J. Yin, Y. Li, Y. Li, M. Xu, Cross-domain fault diagnosis using knowledge transfer strategy: a review, *IEEE Access* 7 (2019) 129260–129290.
- [12] R. Yan, F. Shen, C. Sun, X. Chen, Knowledge transfer for rotary machine fault diagnosis, *IEEE Sensors Journal* (2019).
- [13] R. Zhang, H. Tao, L. Wu, Y. Guan, Transfer learning with neural networks for bearing fault diagnosis in changing working conditions, *IEEE Access* 5 (2017) 14347–14357.
- [14] C. Zhang, L. Xu, X. Li, H. Wang, A method of fault diagnosis for rotary equipment based on deep learning, in: *2018 Prognostics and System Health Management Conference (PHM-Chongqing)*, IEEE, pp. 958–962.
- [15] D. Chen, S. Yang, F. Zhou, Incipient fault diagnosis based on dnn with transfer learning, in: *2018 International Conference on Control, Automation and Information Sciences (ICCAIS)*, IEEE, pp. 303–308.
- [16] M. J. Hasan, M. Sohaib, J.-M. Kim, 1d cnn-based transfer learning model for bearing fault diagnosis under variable working conditions, in: *International Conference on Computational Intelligence in Information System*, Springer, pp. 13–23.
- [17] H. Kim, B. D. Youn, A new parameter repurposing method for parameter transfer with small dataset and its application in fault diagnosis of rolling element bearings, *IEEE Access* 7 (2019) 46917–46930.
- [18] M. J. Hasan, M. M. Islam, J.-M. Kim, Acoustic spectral imaging and transfer learning for reliable bearing fault diagnosis under variable speed conditions, *Measurement* 138 (2019) 620–631.

- [19] C. Sun, M. Ma, Z. Zhao, S. Tian, R. Yan, X. Chen, Deep transfer learning based on sparse autoencoder for remaining useful life prediction of tool in manufacturing, *IEEE Transactions on Industrial Informatics* 15 (2018) 2416–2425.
- [20] S. Shao, S. McAleer, R. Yan, P. Baldi, Highly accurate machine fault diagnosis using deep transfer learning, *IEEE Transactions on Industrial Informatics* 15 (2018) 2446–2455.
- [21] D. Chen, S. Yang, F. Zhou, Transfer learning based fault diagnosis with missing data due to multi-rate sampling, *Sensors* 19 (2019) 1826.
- [22] W. Mao, L. Ding, S. Tian, X. Liang, Online detection for bearing incipient fault based on deep transfer learning, *Measurement* (2019) 107278.
- [23] S. A. Sharaf, Beam pump dynamometer card prediction using artificial neural networks, *KnE Engineering* 3 (2018) 198–212.
- [24] P. Cao, S. Zhang, J. Tang, Preprocessing-free gear fault diagnosis using small datasets with deep convolutional neural network-based transfer learning, *IEEE Access* 6 (2018) 26241–26253.
- [25] J. Wang, Z. Mo, H. Zhang, Q. Miao, A deep learning method for bearing fault diagnosis based on time-frequency image, *IEEE Access* 7 (2019) 42373–42383.
- [26] Z. Chen, K. Gryllias, W. Li, Intelligent fault diagnosis for rotary machinery using transferable convolutional neural network, *IEEE Transactions on Industrial Informatics* (2019).
- [27] D. Iba, Y. Ishii, Y. Tsutsui, N. Miura, T. Iizuka, A. Masuda, A. Sone, I. Moriwaki, Vibration analysis of a meshing gear pair by neural network (visualization of meshing vibration and detection of a crack at tooth root by vgg16 with transfer learning), in: *Smart Structures and NDE for Energy Systems and Industry 4.0*, volume 10973, International Society for Optics and Photonics, p. 109730Y.
- [28] P. Ma, H. Zhang, W. Fan, C. Wang, G. Wen, X. Zhang, A novel bearing fault diagnosis method based on 2d image representation and transfer learning-convolutional neural network, *Measurement Science and Technology* 30 (2019) 055402.
- [29] A. S. Qureshi, A. Khan, A. Zameer, A. Usman, Wind power prediction using deep neural network based meta regression and transfer learning, *Applied Soft Computing* 58 (2017) 742–755.
- [30] S.-s. Zhong, S. Fu, L. Lin, A novel gas turbine fault diagnosis method based on transfer learning with cnn, *Measurement* 137 (2019) 435–453.
- [31] T. Han, C. Liu, W. Yang, D. Jiang, Learning transferable features in deep convolutional neural networks for diagnosing unseen machine conditions, *ISA transactions* (2019).
- [32] G. Xu, M. Liu, Z. Jiang, W. Shen, C. Huang, Online fault diagnosis method based on transfer convolutional neural networks, *IEEE Transactions on Instrumentation and Measurement* (2019).
- [33] W. Dai, Q. Yang, G.-R. Xue, Y. Yu, Boosting for transfer learning, in: *Proceedings of the 24th international conference on Machine learning*, ACM, pp. 193–200.
- [34] Y. Li, N. Wang, J. Shi, J. Liu, X. Hou, Revisiting batch normalization for practical domain adaptation, *arXiv preprint arXiv:1603.04779* (2016).
- [35] D. Xiao, Y. Huang, C. Qin, Z. Liu, Y. Li, C. Liu, Transfer learning with convolutional neural networks for small sample size problem in machinery fault diagnosis, *Proceedings of the Institution of Mechanical Engineers, Part C: Journal of Mechanical Engineering Science* (2019) 0954406219840381.
- [36] W. Zhang, G. Peng, C. Li, Y. Chen, Z. Zhang, A new deep learning model for fault diagnosis with good anti-noise and domain adaptation ability on raw vibration signals, *Sensors* 17 (2017) 425.
- [37] W. Qian, S. Li, J. Wang, A new transfer learning method and its application on rotating machine fault diagnosis under variant working conditions, *IEEE Access* 6 (2018) 69907–69917.
- [38] B. Sun, K. Saenko, Deep coral: Correlation alignment for deep domain adaptation, in: *European Conference on Computer Vision*, Springer, pp. 443–450.
- [39] K. M. Borgwardt, A. Gretton, M. J. Rasch, H.-P. Kriegel, B. Schölkopf, A. J. Smola, Integrating structured biological data by kernel maximum mean discrepancy, *Bioinformatics* 22 (2006) e49–e57.
- [40] D. Sejdinovic, B. Sriperumbudur, A. Gretton, K. Fukumizu, et al., Equivalence of distance-based and rkhs-based statistics in hypothesis testing, *The Annals of Statistics* 41 (2013) 2263–2291.
- [41] A. Gretton, D. Sejdinovic, H. Strathmann, S. Balakrishnan, M. Pontil, K. Fukumizu, B. K. Sriperumbudur, Optimal kernel choice for large-scale two-sample tests, in: *Advances in neural information processing systems*, pp. 1205–1213.
- [42] M. Long, Y. Cao, J. Wang, M. I. Jordan, Learning transferable features with deep adaptation networks, *arXiv preprint arXiv:1502.02791* (2015).
- [43] M. Long, J. Wang, G. Ding, J. Sun, P. S. Yu, Transfer feature learning with joint distribution adaptation, in: *Proceedings of the IEEE international conference on computer vision*, pp. 2200–2207.
- [44] J. Wang, Y. Chen, S. Hao, W. Feng, Z. Shen, Balanced distribution adaptation for transfer learning, in: *2017 IEEE International Conference on Data Mining (ICDM)*, IEEE, pp. 1129–1134.

- [45] M. Long, H. Zhu, J. Wang, M. I. Jordan, Deep transfer learning with joint adaptation networks, in: Proceedings of the 34th International Conference on Machine Learning-Volume 70, JMLR. org, pp. 2208–2217.
- [46] K. Wang, B. Wu, Power equipment fault diagnosis model based on deep transfer learning with balanced distribution adaptation, in: International Conference on Advanced Data Mining and Applications, Springer, pp. 178–188.
- [47] X. Wang, H. He, L. Li, A hierarchical deep domain adaptation approach for fault diagnosis of power plant thermal system, *IEEE Transactions on Industrial Informatics* (2019).
- [48] W. Lu, B. Liang, Y. Cheng, D. Meng, J. Yang, T. Zhang, Deep model based domain adaptation for fault diagnosis, *IEEE Transactions on Industrial Electronics* 64 (2016) 2296–2305.
- [49] B. Zhang, W. Li, X.-L. Li, S.-K. Ng, Intelligent fault diagnosis under varying working conditions based on domain adaptive convolutional neural networks, *IEEE Access* 6 (2018) 66367–66384.
- [50] L. Wen, L. Gao, X. Li, A new deep transfer learning based on sparse auto-encoder for fault diagnosis, *IEEE Transactions on Systems, Man, and Cybernetics: Systems* 49 (2017) 136–144.
- [51] B. Yang, Y. Lei, F. Jia, S. Xing, An intelligent fault diagnosis approach based on transfer learning from laboratory bearings to locomotive bearings, *Mechanical Systems and Signal Processing* 122 (2019) 692–706.
- [52] S. Tang, H. Tang, M. Chen, Transfer-learning based gas path analysis method for gas turbines, *Applied Thermal Engineering* 155 (2019) 1–13.
- [53] X. Li, W. Zhang, Q. Ding, Cross-domain fault diagnosis of rolling element bearings using deep generative neural networks, *IEEE Transactions on Industrial Electronics* 66 (2018) 5525–5534.
- [54] Y. Xu, Y. Sun, X. Liu, Y. Zheng, A digital-twin-assisted fault diagnosis using deep transfer learning, *IEEE Access* 7 (2019) 19990–19999.
- [55] Z. Tong, W. Li, B. Zhang, M. Zhang, Bearing fault diagnosis based on domain adaptation using transferable features under different working conditions, *Shock and Vibration* 2018 (2018).
- [56] Z. Tong, W. Li, B. Zhang, F. Jiang, G. Zhou, Bearing fault diagnosis under variable working conditions based on domain adaptation using feature transfer learning, *IEEE Access* 6 (2018) 76187–76197.
- [57] X. Li, W. Zhang, Q. Ding, A robust intelligent fault diagnosis method for rolling element bearings based on deep distance metric learning, *Neurocomputing* 310 (2018) 77–95.
- [58] B. Yang, Y. Lei, F. Jia, S. Xing, A transfer learning method for intelligent fault diagnosis from laboratory machines to real-case machines, in: 2018 International Conference on Sensing, Diagnostics, Prognostics, and Control (SDPC), IEEE, pp. 35–40.
- [59] Z. An, S. Li, J. Wang, Y. Xin, K. Xu, Generalization of deep neural network for bearing fault diagnosis under different working conditions using multiple kernel method, *Neurocomputing* 352 (2019) 42–53.
- [60] X. Li, W. Zhang, Q. Ding, J.-Q. Sun, Multi-layer domain adaptation method for rolling bearing fault diagnosis, *Signal Processing* 157 (2019) 180–197.
- [61] T. Han, C. Liu, W. Yang, D. Jiang, Deep transfer network with joint distribution adaptation: a new intelligent fault diagnosis framework for industry application, *ISA transactions* (2019).
- [62] W. Qian, S. Li, P. Yi, K. Zhang, A novel transfer learning method for robust fault diagnosis of rotating machines under variable working conditions, *Measurement* 138 (2019) 514–525.
- [63] Y. Ganin, E. Ustinova, H. Ajakan, P. Germain, H. Larochelle, F. Laviolette, M. Marchand, V. Lempitsky, Domain-adversarial training of neural networks, *The Journal of Machine Learning Research* 17 (2016) 2096–2030.
- [64] E. Tzeng, J. Hoffman, K. Saenko, T. Darrell, Adversarial discriminative domain adaptation, in: Proceedings of the IEEE Conference on Computer Vision and Pattern Recognition, pp. 7167–7176.
- [65] B. Zhang, W. Li, J. Hao, X.-L. Li, M. Zhang, Adversarial adaptive 1-d convolutional neural networks for bearing fault diagnosis under varying working condition, arXiv preprint arXiv:1805.00778 (2018).
- [66] T. Han, C. Liu, W. Yang, D. Jiang, A novel adversarial learning framework in deep convolutional neural network for intelligent diagnosis of mechanical faults, *Knowledge-Based Systems* 165 (2019) 474–487.
- [67] L. Guo, Y. Lei, S. Xing, T. Yan, N. Li, Deep convolutional transfer learning network: A new method for intelligent fault diagnosis of machines with unlabeled data, *IEEE Transactions on Industrial Electronics* 66 (2018) 7316–7325.
- [68] Q. Wang, G. Michau, O. Fink, Domain adaptive transfer learning for fault diagnosis, arXiv preprint arXiv:1905.06004 (2019).
- [69] C. Cheng, B. Zhou, G. Ma, D. Wu, Y. Yuan, Wasserstein distance based deep adversarial transfer learning for intelligent fault diagnosis, arXiv preprint arXiv:1903.06753 (2019).
- [70] Y. Xie, T. Zhang, A transfer learning strategy for rotation machinery fault diagnosis based on cycle-consistent generative adversarial networks, in:

2018 Chinese Automation Congress (CAC), IEEE, pp. 1309–1313.

- [71] Y. LeCun, Y. Bengio, et al., Convolutional networks for images, speech, and time series, *The handbook of brain theory and neural networks* 3361 (1995) 1995.
- [72] K. Simonyan, A. Zisserman, Very deep convolutional networks for large-scale image recognition, *arXiv preprint arXiv:1409.1556* (2014).
- [73] C. Szegedy, W. Liu, Y. Jia, P. Sermanet, S. Reed, D. Anguelov, D. Erhan, V. Vanhoucke, A. Rabinovich, Going deeper with convolutions, in: *Proceedings of the IEEE conference on computer vision and pattern recognition*, pp. 1–9.
- [74] K. He, X. Zhang, S. Ren, J. Sun, Deep residual learning for image recognition, in: *Proceedings of the IEEE conference on computer vision and pattern recognition*, pp. 770–778.
- [75] S. Ioffe, C. Szegedy, Batch normalization: Accelerating deep network training by reducing internal covariate shift, *arXiv preprint arXiv:1502.03167* (2015).
- [76] S. J. Pan, I. W. Tsang, J. T. Kwok, Q. Yang, Domain adaptation via transfer component analysis, *IEEE Transactions on Neural Networks* 22 (2010) 199–210.
- [77] E. Tzeng, J. Hoffman, N. Zhang, K. Saenko, T. Darrell, Deep domain confusion: Maximizing for domain invariance, *arXiv preprint arXiv:1412.3474* (2014).
- [78] B. Sun, J. Feng, K. Saenko, Return of frustratingly easy domain adaptation, in: *Thirtieth AAAI Conference on Artificial Intelligence*.
- [79] M. Long, Z. Cao, J. Wang, M. I. Jordan, Conditional adversarial domain adaptation, in: *Advances in Neural Information Processing Systems*, pp. 1640–1650.
- [80] Case Western Reserve University, Case Western Reserve University (CWRU) Bearing Data Center, [Online], Available: <https://csegroups.case.edu/bearingdatacenter/pages/download-data-file/>, accessed on August 2019.
- [81] C. Lessmeier, J. K. Kimotho, D. Zimmer, W. Sextro, Condition monitoring of bearing damage in electromechanical drive systems by using motor current signals of electric motors: A benchmark data set for data-driven classification, in: *Proceedings of the European conference of the prognostics and health management society*, pp. 05–08.
- [82] C. Lessmeier, et al. KAT-DataCenter, Chair of Design and Drive Technology, Paderborn University, Available: <https://mb.uni-paderborn.de/kat/forschung/datacenter/bearing-datacenter/>, accessed on August 2019.
- [83] K. Li, School of Mechanical Engineering, Jiangnan University, Available: <http://mad-net.org:8765/explore.html?t=0.5831516555847212.>, accessed on August 2019.
- [84] K. Li, X. Ping, H. Wang, P. Chen, Y. Cao, Sequential fuzzy diagnosis method for motor roller bearing in variable operating conditions based on vibration analysis, *Sensors* 13 (2013) 8013–8041.
- [85] PHMSociety, PHM09 Data Challenge, Available: <https://www.phmsociety.org/competition/PHM/09/apparatus>, accessed on August 2019.
- [86] S. Shao, S. McAleer, R. Yan, P. Baldi, Mechanical dataset, Available: <http://mlmechanics.ics.uci.edu/>, accessed on August 2019.
- [87] X. Glorot, A. Bordes, Y. Bengio, Domain adaptation for large-scale sentiment classification: A deep learning approach, in: *Proceedings of the 28th international conference on machine learning (ICML-11)*, pp. 513–520.
- [88] J. Yosinski, J. Clune, Y. Bengio, H. Lipson, How transferable are features in deep neural networks?, in: *Advances in neural information processing systems*, pp. 3320–3328.
- [89] M. D. Zeiler, R. Fergus, Visualizing and understanding convolutional networks, in: *European conference on computer vision*, Springer, pp. 818–833.
- [90] R. R. Selvaraju, M. Cogswell, A. Das, R. Vedantam, D. Parikh, D. Batra, Grad-cam: Visual explanations from deep networks via gradient-based localization, in: *Proceedings of the IEEE International Conference on Computer Vision*, pp. 618–626.
- [91] A. Vaswani, N. Shazeer, N. Parmar, J. Uszkoreit, L. Jones, A. N. Gomez, Ł. Kaiser, I. Polosukhin, Attention is all you need, in: *Advances in neural information processing systems*, pp. 5998–6008.

Appendix A. Evaluation Results

CWRU with the time domain input

Task	Loc	Basis		AdaBN		MK-MMD		JMMD		CORAL		DANN		CDAN	
		Max	Mean	Max	Mean	Max	Mean	Max	Mean	Max	Mean	Max	Mean	Max	Mean
0-1	Best	100.00	99.91	100.00	99.91	100.00	100.00	100.00	100.00	100.00	99.55	100.00	100.00	100.00	100.00
	Last	99.48	99.12	100.00	99.77	100.00	98.51	100.00	100.00	100.00	96.75	100.00	99.94	100.00	100.00
0-2	Best	99.94	98.73	100.00	99.77	100.00	100.00	100.00	100.00	100.00	97.01	100.00	100.00	100.00	100.00
	Last	96.30	94.07	99.74	99.26	100.00	99.74	100.00	99.61	100.00	94.80	100.00	100.00	100.00	100.00
0-3	Best	98.32	93.15	98.77	96.96	99.68	97.09	100.00	100.00	99.03	92.69	100.00	100.00	100.00	99.29
	Last	92.42	86.92	94.69	92.20	99.35	93.72	100.00	99.68	96.76	90.87	100.00	100.00	100.00	96.89
1-0	Best	99.92	99.86	99.92	98.04	100.00	99.85	100.00	100.00	100.00	99.46	100.00	100.00	100.00	100.00
	Last	99.77	99.48	98.08	94.07	93.87	93.33	100.00	98.54	99.62	95.33	100.00	99.92	100.00	100.00
1-2	Best	100.00	100.00	99.94	99.48	100.00	100.00	100.00	100.00	100.00	100.00	100.00	100.00	100.00	100.00
	Last	99.94	99.87	99.87	96.60	100.00	100.00	100.00	100.00	100.00	99.87	100.00	100.00	100.00	100.00
1-3	Best	99.68	98.59	97.93	96.02	100.00	100.00	100.00	100.00	100.00	95.79	100.00	100.00	100.00	100.00
	Last	98.32	94.33	96.18	90.93	100.00	99.94	100.00	100.00	99.68	93.79	100.00	99.94	100.00	99.87
2-0	Best	99.23	98.36	97.16	92.69	99.62	99.39	100.00	99.92	99.23	97.24	100.00	99.77	99.62	99.54
	Last	98.70	96.25	96.70	85.13	98.47	93.72	100.00	99.62	97.32	95.02	99.62	99.31	99.62	99.31
2-1	Best	99.42	99.25	99.61	99.05	100.00	99.68	100.00	100.00	99.68	98.51	100.00	99.74	100.00	99.87
	Last	98.31	97.35	98.25	97.04	100.00	99.61	100.00	99.74	98.70	97.92	100.00	99.55	100.00	99.55
2-3	Best	99.94	99.45	99.03	98.30	100.00	100.00	100.00	100.00	100.00	99.22	100.00	100.00	100.00	100.00
	Last	99.87	97.78	98.90	96.43	100.00	100.00	100.00	100.00	100.00	98.90	100.00	100.00	100.00	100.00
3-0	Best	91.26	87.11	95.40	89.91	99.23	98.93	100.00	99.54	94.25	87.89	99.62	99.00	99.62	99.39
	Last	87.36	81.10	95.33	84.12	95.02	92.18	100.00	98.85	93.49	85.44	99.23	98.54	99.23	98.77
3-1	Best	91.55	88.51	96.82	95.34	100.00	99.22	100.00	99.68	97.73	96.23	100.00	99.74	100.00	98.12
	Last	88.04	82.83	94.09	89.53	100.00	99.09	100.00	99.09	97.40	95.52	100.00	99.42	100.00	97.53
3-2	Best	99.61	97.82	99.87	99.82	100.00	100.00	100.00	100.00	100.00	97.79	100.00	100.00	100.00	100.00
	Last	96.23	90.12	99.03	96.52	100.00	100.00	100.00	100.00	99.68	97.14	100.00	99.94	100.00	99.94
Best average		98.24	96.73	98.70	97.11	99.88	99.51	100.00	99.93	99.16	96.78	99.97	99.86	99.94	99.68
Last average		96.23	93.27	97.57	93.47	98.89	97.49	100.00	99.60	98.55	95.11	99.90	99.71	99.90	99.32
Best bias		0.00	0.00	0.47	0.38	1.64	2.78	1.76	3.20	0.92	0.05	1.73	3.13	1.70	2.96
Last bias		0.00	0.00	1.34	0.20	2.66	4.22	3.77	6.33	2.33	1.84	3.68	6.44	3.68	6.05

CWRU with the frequency domain input

Task	Loc	Basis		AdaBN		MK-MMD		JMMD		CORAL		DANN		CDAN	
		Max	Mean	Max	Mean	Max	Mean	Max	Mean	Max	Mean	Max	Mean	Max	Mean
0-1	Best	99.61	99.46	99.48	99.13	100.00	99.94	100.00	100.00	99.87	100.00	99.94	100.00	100.00	100.00
	Last	99.48	98.60	98.64	98.25	100.00	99.81	100.00	99.48	100.00	99.81	100.00	99.87	99.68	99.61
0-2	Best	90.51	89.87	91.03	90.27	100.00	100.00	100.00	99.94	100.00	98.12	100.00	99.81	100.00	95.52
	Last	89.34	86.16	89.15	87.86	100.00	99.87	100.00	98.90	100.00	97.92	100.00	99.55	100.00	92.73
0-3	Best	77.40	76.64	83.55	80.06	100.00	95.54	100.00	97.73	98.06	93.07	100.00	94.95	100.00	93.85
	Last	75.78	74.22	78.04	75.35	100.00	94.89	100.00	96.57	97.41	91.07	99.68	91.98	100.00	93.66
1-0	Best	98.01	96.89	97.78	97.35	100.00	99.31	100.00	99.39	98.85	98.39	100.00	99.31	100.00	99.54
	Last	96.17	94.53	96.93	94.37	93.49	91.42	99.62	96.32	98.08	97.16	99.23	98.85	98.08	97.78
1-2	Best	97.01	93.01	95.00	93.39	100.00	100.00	100.00	100.00	100.00	99.29	100.00	100.00	100.00	99.68
	Last	93.63	91.19	90.58	89.66	100.00	100.00	100.00	100.00	100.00	98.83	100.00	100.00	100.00	98.90
1-3	Best	83.10	81.35	81.15	79.73	100.00	96.96	100.00	94.63	99.68	98.12	100.00	99.94	100.00	97.86
	Last	77.33	75.53	77.66	73.99	100.00	96.64	99.68	93.59	99.35	97.86	100.00	99.81	100.00	96.57
2-0	Best	82.61	78.55	80.54	79.11	94.64	89.43	99.62	92.41	97.70	90.65	97.70	90.35	90.80	89.50
	Last	80.61	70.25	77.24	68.69	89.27	85.75	94.25	83.14	97.32	89.89	97.32	88.35	89.27	86.21
2-1	Best	91.75	89.24	90.45	88.68	92.21	90.72	100.00	94.09	99.03	95.91	100.00	98.12	92.53	90.45
	Last	87.33	85.66	86.22	83.72	86.04	85.39	100.00	90.78	98.05	94.67	99.35	96.24	92.53	86.30
2-3	Best	89.05	86.61	93.52	87.72	100.00	93.59	100.00	100.00	100.00	98.00	89.32	86.93	100.00	90.03
	Last	79.08	77.53	91.52	79.69	100.00	90.68	100.00	100.00	100.00	97.41	85.11	84.01	100.00	87.38
3-0	Best	77.78	74.15	76.48	74.16	95.02	88.43	87.74	84.90	83.52	81.23	97.32	88.28	87.74	81.07
	Last	72.95	64.84	72.03	69.40	90.04	84.98	83.52	78.39	82.76	79.69	96.93	84.60	86.97	79.00
3-1	Best	80.25	77.52	83.30	79.49	100.00	99.94	100.00	95.65	98.05	90.91	100.00	90.85	85.06	83.70
	Last	72.45	70.59	80.70	73.90	100.00	99.81	100.00	93.64	97.73	89.48	99.68	87.92	84.74	82.40
3-2	Best	91.62	89.64	95.06	89.97	100.00	90.19	100.00	95.97	100.00	98.90	100.00	95.32	100.00	94.74
	Last	84.28	78.95	84.67	79.27	100.00	84.61	100.00	93.83	100.00	97.79	100.00	93.70	100.00	92.14
Best average		88.23	86.08	88.95	86.59	98.49	95.34	98.95	96.22	97.91	95.21	98.70	95.32	96.34	93.00
Last average		84.04	80.67	85.28	81.18	96.57	92.82	98.09	93.72	97.56	94.30	98.11	93.74	95.94	91.06
Best bias		0.00	0.00	0.72	0.51	10.26	9.26	10.72	10.14	9.68	9.13	10.47	9.24	8.12	6.92
Last bias		0.00	0.00	1.25	0.51	12.53	12.15	14.05	13.05	13.52	13.63	14.07	13.07	11.90	10.39

PU with the time domain input

Task	Loc	Basis		AdaBN		MK-MMD		JMMD		CORAL		DANN		CDAN	
		Max	Mean	Max	Mean	Max	Mean	Max	Mean	Max	Mean	Max	Mean	Max	Mean
0-1	Best	24.16	21.44	40.04	38.26	36.81	33.10	37.88	36.50	31.13	27.97	44.17	41.72	38.04	37.02
	Last	15.54	14.02	33.59	30.00	32.36	29.14	35.43	32.79	29.75	24.69	40.64	38.19	36.35	33.68
0-2	Best	79.24	77.78	76.83	74.70	82.29	80.73	82.44	80.61	76.18	69.89	83.05	80.95	81.83	79.85
	Last	78.60	76.33	75.91	72.27	81.37	79.48	81.98	79.63	57.10	40.46	83.05	79.97	80.15	78.56
0-3	Best	47.90	45.02	51.23	48.93	47.66	43.84	54.46	52.68	49.47	39.61	57.03	55.04	54.01	50.05
	Last	32.24	30.02	41.54	40.26	44.18	41.09	52.95	50.92	38.58	33.19	55.98	53.74	51.89	47.62
1-0	Best	33.43	30.55	50.02	46.56	38.71	35.85	43.16	40.77	27.80	23.50	42.24	38.99	39.02	36.31
	Last	27.99	23.57	41.41	38.27	37.48	33.24	36.71	35.94	18.13	15.61	40.25	35.42	35.33	30.75
1-2	Best	34.48	33.13	49.80	44.92	41.68	38.23	47.63	41.19	32.06	25.53	45.80	43.88	46.56	44.43
	Last	26.02	24.18	43.17	37.13	40.00	35.39	43.97	35.17	28.70	21.16	41.83	39.57	43.51	38.99
1-3	Best	23.74	22.34	34.91	32.89	28.14	26.51	30.71	28.68	20.88	19.15	36.01	32.19	34.34	30.98
	Last	19.74	16.09	30.46	25.36	25.42	23.39	24.96	22.54	17.85	14.37	29.80	27.05	27.84	23.63
2-0	Best	79.08	77.70	74.75	73.99	80.80	78.86	80.65	78.93	76.19	72.63	81.41	80.27	82.95	80.40
	Last	78.43	76.73	72.84	71.35	79.57	77.79	79.88	77.30	64.82	50.41	80.18	79.20	81.87	79.11
2-1	Best	26.04	23.16	35.52	33.16	36.50	35.03	38.96	36.72	33.74	29.94	41.26	39.27	45.55	41.38
	Last	16.24	14.71	27.33	25.05	34.66	31.07	33.59	32.06	31.90	26.59	39.11	36.53	38.65	34.76
2-3	Best	45.41	43.05	50.29	49.61	46.44	43.90	51.29	50.05	38.12	33.89	53.86	50.62	51.59	49.53
	Last	32.70	31.23	44.02	40.73	46.14	41.94	49.62	47.66	25.11	18.85	52.04	49.23	50.23	47.44
3-0	Best	45.75	42.35	48.73	46.88	48.39	44.02	54.69	51.12	32.87	31.52	50.38	49.62	51.77	48.69
	Last	36.01	32.16	45.16	40.94	45.62	41.66	53.92	49.31	24.73	17.23	49.62	47.93	45.62	43.90
3-1	Best	31.01	29.25	34.51	32.65	30.06	29.17	30.67	29.29	28.83	26.41	33.59	31.50	33.28	31.59
	Last	26.59	25.27	32.05	28.43	28.22	22.64	27.61	23.53	17.18	14.23	30.67	27.45	30.67	27.97
3-2	Best	43.53	40.23	52.37	48.58	44.12	43.54	51.60	49.01	32.67	30.56	52.82	49.37	47.33	45.25
	Last	35.68	32.39	46.22	41.99	38.47	37.19	49.77	47.39	22.14	18.93	50.84	47.57	42.75	40.40
Best average		42.81	40.50	49.92	47.59	46.80	44.40	50.35	47.96	40.00	35.88	51.80	49.45	50.52	47.96
Last average		35.48	33.06	44.48	40.98	44.46	41.17	47.53	44.52	31.33	24.64	49.50	46.82	47.07	43.90
Best bias		0.00	0.00	7.10	7.09	3.99	3.90	7.53	7.46	-2.82	-4.62	8.99	8.95	7.71	7.46
Last bias		0.00	0.00	8.99	7.92	8.98	8.11	12.05	11.46	-4.15	-8.41	14.02	13.76	11.59	10.84

PU with the frequency domain input

Task	Loc	Basis		AdaBN		MK-MMD		JMMD		CORAL		DANN		CDAN	
		Max	Mean	Max	Mean	Max	Mean	Max	Mean	Max	Mean	Max	Mean	Max	Mean
0-1	Best	24.87	23.28	33.77	30.21	34.97	32.79	39.72	36.19	26.84	23.44	44.48	42.91	42.48	40.06
	Last	22.72	20.96	26.80	24.15	34.36	30.43	36.96	33.28	24.54	19.45	43.56	40.34	40.18	35.46
0-2	Best	93.21	92.08	92.27	90.63	94.96	94.35	96.34	95.54	88.70	85.83	95.42	94.29	97.25	95.36
	Last	91.93	90.87	91.56	89.12	94.50	93.59	95.57	94.99	82.29	66.47	94.96	93.71	96.64	94.72
0-3	Best	62.91	61.18	64.21	60.93	77.76	76.67	80.33	78.55	60.36	57.76	84.72	82.99	83.51	80.63
	Last	58.95	57.14	61.64	57.11	77.31	75.04	79.12	77.40	54.01	50.83	84.27	82.15	82.00	79.49
1-0	Best	29.31	27.65	28.08	26.91	32.57	30.51	34.41	31.58	23.66	21.87	34.56	32.29	36.56	33.12
	Last	26.76	25.13	25.59	24.61	27.50	26.27	29.19	28.02	14.59	12.81	30.88	28.48	34.56	29.37
1-2	Best	27.03	26.58	25.22	24.49	32.67	30.87	40.76	33.86	25.50	23.76	38.78	36.91	45.50	40.31
	Last	25.44	24.14	23.08	21.50	30.23	27.33	39.39	30.44	18.78	15.39	38.02	35.27	44.89	38.51
1-3	Best	19.53	18.03	20.35	19.04	23.90	22.03	26.32	24.18	20.27	15.95	26.93	24.84	28.59	26.63
	Last	14.17	13.75	15.74	14.74	21.33	20.36	24.21	22.30	12.56	11.10	25.57	22.88	27.53	21.39
2-0	Best	88.69	87.79	89.59	88.98	92.32	91.46	94.32	91.89	83.72	82.34	94.16	93.09	94.01	93.27
	Last	87.47	86.40	88.91	88.37	91.40	90.48	93.86	91.37	79.88	64.82	94.01	92.50	93.09	92.57
2-1	Best	26.83	24.49	28.43	27.47	36.96	33.56	44.33	40.06	32.98	29.48	53.07	47.36	50.15	48.44
	Last	22.57	20.55	23.98	22.43	35.28	32.30	43.87	37.27	29.14	24.11	51.69	46.01	49.08	46.23
2-3	Best	63.25	60.23	62.28	60.62	79.58	77.40	79.27	76.97	66.26	60.33	83.36	80.21	82.60	79.15
	Last	60.55	57.18	59.16	58.10	78.67	76.70	78.52	76.31	64.30	43.90	83.06	79.52	81.54	78.24
3-0	Best	58.00	56.25	60.18	56.28	62.52	60.06	74.81	71.58	52.53	51.33	80.03	69.40	67.74	63.29
	Last	54.78	52.58	54.75	51.63	61.14	58.77	74.04	71.03	50.69	36.80	78.96	68.76	65.90	61.50
3-1	Best	25.85	24.21	30.33	29.52	40.03	32.18	34.66	31.87	24.54	22.36	30.67	29.97	39.57	35.52
	Last	21.80	20.90	26.90	24.76	39.72	30.15	30.67	23.04	19.48	16.20	28.53	24.57	37.88	32.12
3-2	Best	59.22	56.57	61.88	56.15	71.91	67.18	81.22	71.39	63.21	55.91	83.82	77.19	79.69	69.56
	Last	56.86	53.64	57.78	54.00	70.69	66.32	81.07	70.47	60.61	48.70	83.36	76.15	78.47	66.47
Best average		48.23	46.53	49.72	47.60	56.68	54.09	60.54	56.97	47.38	44.20	62.50	59.29	62.30	58.78
Last average		45.33	43.60	46.32	44.21	55.18	52.31	58.87	54.66	42.57	34.22	61.41	57.53	60.98	56.34
Best bias		0.00	0.00	1.49	1.07	8.45	7.56	12.32	10.45	-0.84	-2.33	14.28	12.76	14.08	12.25
Last bias		0.00	0.00	0.99	0.61	9.84	8.71	13.54	11.06	-2.76	-9.39	16.07	13.93	15.65	12.74

JNU with the time domain input

Task	Loc	Basis		AdaBN		MK-MMD		JMMD		CORAL		DANN		CDAN	
		Max	Mean	Max	Mean	Max	Mean	Max	Mean	Max	Mean	Max	Mean	Max	Mean
0-1	Best	99.04	98.85	98.46	97.70	99.32	99.08	99.83	99.15	95.73	93.75	98.98	98.88	99.32	99.22
	Last	97.92	97.54	95.97	95.29	98.81	98.33	98.46	97.95	72.35	61.74	98.12	97.54	98.12	97.85
0-2	Best	96.42	95.86	96.66	96.22	98.46	98.19	98.81	98.29	95.22	92.53	98.29	97.68	97.95	97.81
	Last	93.72	92.80	93.58	93.19	97.78	97.20	97.95	97.27	55.46	52.18	97.27	96.69	97.10	96.79
1-0	Best	89.49	87.87	91.60	91.16	97.78	96.96	97.95	97.17	77.65	72.15	96.25	95.26	95.39	94.30
	Last	68.87	66.31	86.89	85.45	97.27	96.21	97.61	96.59	73.38	61.74	96.08	94.85	94.20	91.50
1-2	Best	98.63	98.29	98.23	97.56	99.66	99.49	99.66	99.49	99.32	97.82	99.49	99.29	99.66	99.42
	Last	98.16	97.77	96.79	95.23	99.32	99.01	99.49	99.11	72.01	58.23	99.32	98.87	98.98	98.60
2-0	Best	91.43	90.73	92.39	90.81	93.86	93.07	94.03	92.93	89.25	85.39	92.66	91.84	93.00	91.81
	Last	87.34	85.94	87.37	83.28	93.17	91.98	93.17	91.78	55.46	53.58	91.64	90.51	91.13	89.56
2-1	Best	99.15	98.89	98.16	97.69	99.49	99.22	99.66	99.35	97.44	96.11	99.15	98.84	99.32	99.18
	Last	98.57	97.62	94.71	94.16	98.29	97.78	98.81	98.46	79.69	56.59	98.63	97.98	98.81	98.50
Best average		95.69	95.08	95.92	95.19	98.10	97.67	98.32	97.73	92.44	89.62	97.47	96.96	97.44	96.96
Last average		90.76	89.67	92.55	91.10	97.44	96.75	97.58	96.86	68.06	57.34	96.84	96.08	96.39	95.47
Best bias		0.00	0.00	0.22	0.11	2.40	2.59	2.63	2.65	-3.26	-5.46	1.78	1.88	1.75	1.88
Last bias		0.00	0.00	1.79	1.44	6.68	7.09	6.82	7.20	-22.71	-32.32	6.08	6.41	5.63	5.80

JNU with the frequency domain input

Task	Loc	Basis		AdaBN		MK-MMD		JMMD		CORAL		DANN		CDAN	
		Max	Mean	Max	Mean	Max	Mean	Max	Mean	Max	Mean	Max	Mean	Max	Mean
0-1	Best	89.80	83.83	84.68	83.59	97.44	96.90	97.44	97.00	82.94	72.97	96.25	93.48	97.44	93.00
	Last	76.38	73.04	82.18	77.77	97.10	96.35	96.42	96.08	60.58	54.95	95.73	92.76	96.42	91.94
0-2	Best	78.19	76.39	73.65	72.43	96.93	95.80	97.78	96.31	71.67	62.59	94.88	90.65	95.39	91.67
	Last	68.57	62.19	61.23	58.66	96.76	95.22	97.27	95.63	71.67	57.92	93.86	88.16	94.20	89.73
1-0	Best	73.75	69.38	84.10	79.58	92.15	87.92	93.34	89.31	67.41	59.97	92.83	91.78	92.83	92.22
	Last	66.79	55.33	76.25	66.58	91.30	85.87	92.83	87.06	60.24	53.62	91.47	90.82	92.15	91.43
1-2	Best	89.93	87.88	87.68	86.61	96.93	96.32	97.61	97.24	83.96	80.89	97.10	96.35	96.93	96.31
	Last	87.37	84.51	84.91	83.17	96.42	95.57	96.93	96.21	77.47	59.93	96.59	95.56	96.42	95.80
2-0	Best	85.53	84.44	85.87	84.31	92.83	92.18	93.86	92.22	79.86	70.99	92.83	90.85	91.13	90.51
	Last	80.44	77.07	81.57	80.02	91.98	91.16	92.15	90.68	60.92	55.29	91.81	89.97	90.61	89.69
2-1	Best	88.84	88.35	88.12	87.79	97.44	95.32	97.95	91.67	91.47	88.19	92.15	90.92	90.61	89.90
	Last	87.92	87.17	86.48	86.10	96.93	94.71	97.61	89.59	91.30	72.22	90.44	89.05	90.10	89.32
Best average		84.34	81.71	84.02	82.38	95.62	94.07	96.33	93.96	79.55	72.60	94.34	92.34	94.06	92.27
Last average		77.91	73.22	78.77	75.38	95.08	93.15	95.54	92.54	70.36	58.99	93.32	91.05	93.32	91.32
Best bias		0.00	0.00	-0.32	0.67	11.28	12.36	11.99	12.25	-4.79	-9.11	10.00	10.63	9.72	10.56
Last bias		0.00	0.00	0.86	2.16	17.17	19.93	17.62	19.32	-7.55	-14.23	15.41	17.83	15.41	18.10

PHM with the time domain input

Task	Loc	Basis		AdaBN		MK-MMD		JMMD		CORAL		DANN		CDAN	
		Max	Mean	Max	Mean	Max	Mean	Max	Mean	Max	Mean	Max	Mean	Max	Mean
0-1	Best	41.60	40.70	41.35	41.04	43.27	41.41	46.79	44.42	39.74	37.50	46.47	44.04	43.59	42.82
	Last	40.06	38.31	39.87	38.32	40.06	37.37	46.79	42.63	31.73	27.69	44.55	41.28	41.67	38.91
0-2	Best	45.90	42.12	46.86	45.67	49.04	45.77	47.44	45.90	39.42	34.74	49.36	46.54	47.44	44.42
	Last	38.14	36.91	43.53	42.66	47.76	42.05	45.83	43.46	30.45	26.15	45.19	42.76	42.95	40.45
0-3	Best	38.46	35.22	43.01	41.72	41.99	38.91	41.99	40.13	33.33	31.34	42.63	40.58	41.99	38.65
	Last	30.77	29.59	39.94	38.01	38.46	35.58	39.42	37.37	27.88	23.08	41.03	37.88	40.71	36.09
1-0	Best	41.92	41.20	42.69	41.27	48.40	45.96	48.08	46.99	41.99	38.14	46.79	45.38	48.08	45.77
	Last	39.17	38.01	38.78	37.68	46.47	41.47	45.19	44.36	31.73	23.46	45.19	42.12	45.83	43.65
1-2	Best	53.85	53.13	54.62	53.44	58.33	56.28	57.37	56.73	53.85	51.28	58.01	56.67	58.01	55.90
	Last	51.60	50.68	53.46	50.87	55.77	51.67	56.73	54.10	43.91	28.65	54.49	52.76	55.13	52.50
1-3	Best	52.05	50.08	52.44	50.81	52.88	50.83	51.92	50.45	47.76	43.40	50.96	49.29	50.96	49.55
	Last	47.12	44.85	46.15	44.91	47.44	45.32	48.40	46.99	40.38	34.42	47.76	44.62	46.47	44.68
2-0	Best	43.14	41.94	44.49	43.41	45.51	44.81	48.08	45.26	37.50	36.09	50.00	44.94	45.51	43.85
	Last	37.18	35.79	39.81	38.11	44.23	40.70	45.83	41.28	27.88	23.85	46.79	41.34	42.31	40.00
2-1	Best	53.01	52.42	53.53	51.65	58.97	54.23	55.13	53.91	45.51	42.69	56.73	53.85	58.97	54.81
	Last	50.83	48.15	50.51	48.06	57.69	51.22	50.64	49.10	37.50	33.72	54.49	49.87	55.13	48.78
2-3	Best	58.78	57.23	58.85	57.36	61.54	59.94	61.54	59.10	52.56	50.64	60.90	58.65	61.22	58.59
	Last	55.38	53.95	56.41	54.82	58.97	57.11	59.62	57.18	41.03	35.25	58.01	55.32	56.09	53.72
3-0	Best	39.23	35.95	41.92	40.13	39.10	38.14	39.74	38.65	34.29	28.91	42.31	39.93	41.67	39.55
	Last	29.10	27.31	38.85	35.69	33.97	32.37	33.01	30.07	25.00	19.30	33.97	32.63	33.65	32.63
3-1	Best	51.47	48.96	51.09	50.17	50.00	46.73	51.28	48.53	43.59	42.18	50.00	49.62	50.96	49.30
	Last	43.27	41.67	47.69	45.39	44.55	42.05	47.44	44.68	38.14	35.06	45.83	42.76	46.47	44.10
3-2	Best	55.13	54.06	57.56	55.40	55.13	53.85	58.01	56.47	51.92	47.11	57.05	55.90	56.09	54.75
	Last	52.18	50.65	52.82	51.26	51.92	50.26	55.13	54.23	41.03	36.79	54.49	52.50	53.53	48.91
Best average		47.88	46.08	49.03	47.67	50.35	48.07	50.61	48.88	43.46	40.34	50.93	48.78	50.37	48.16
Last average		42.90	41.32	45.65	43.82	47.27	43.93	47.84	45.45	34.72	28.95	47.65	44.65	46.66	43.70
Best bias		0.00	0.00	1.16	1.59	2.47	1.99	2.74	2.79	-4.42	-5.75	3.06	2.70	2.50	2.08
Last bias		0.00	0.00	2.75	2.49	4.37	2.61	4.94	4.13	-8.18	-12.37	4.75	3.33	3.76	2.38

PHM with the frequency domain input

Task	Loc	Basis		AdaBN		MK-MMD		JMMD		CORAL		DANN		CDAN	
		Max	Mean	Max	Mean	Max	Mean	Max	Mean	Max	Mean	Max	Mean	Max	Mean
0-1	Best	54.87	53.96	57.12	55.13	63.78	61.41	63.14	61.09	57.69	54.10	63.78	61.86	67.31	63.59
	Last	51.09	49.71	51.41	50.77	62.18	58.66	60.58	58.27	56.73	45.32	61.22	57.18	66.03	61.99
0-2	Best	51.67	49.13	48.40	46.96	53.53	50.71	53.21	51.35	55.13	46.86	52.24	50.26	57.37	52.82
	Last	43.97	40.39	43.14	40.92	48.72	46.09	49.68	47.95	47.12	39.04	47.44	44.81	54.49	48.40
0-3	Best	45.19	43.04	44.49	41.98	48.40	46.79	48.72	47.63	44.55	43.14	46.15	45.06	50.32	46.35
	Last	32.76	28.40	38.14	36.32	43.59	40.26	44.23	42.37	41.03	38.98	42.63	40.00	47.76	40.58
1-0	Best	60.13	56.13	58.21	55.16	67.31	64.30	72.44	67.56	57.69	53.27	71.79	65.45	65.38	64.36
	Last	54.94	52.54	55.13	52.94	63.46	61.99	68.91	63.97	57.05	48.65	69.55	63.78	63.78	62.18
1-2	Best	66.99	64.27	65.00	63.54	67.31	64.49	68.91	65.00	68.59	61.47	69.55	66.92	66.99	66.48
	Last	60.00	59.58	63.08	60.28	63.78	61.28	62.82	60.64	66.03	53.85	68.27	64.74	66.67	64.81
1-3	Best	62.24	60.15	67.69	64.77	58.01	56.28	61.22	59.55	58.01	53.91	60.90	59.36	66.03	61.73
	Last	57.50	54.90	64.42	61.52	55.45	51.92	57.69	54.94	53.53	48.21	58.65	56.28	61.86	58.78
2-0	Best	53.08	49.88	55.00	53.79	59.94	56.54	60.90	58.08	52.88	46.86	62.50	60.51	62.18	59.87
	Last	44.29	41.54	49.87	45.59	56.09	54.43	58.01	54.36	37.50	33.84	60.58	58.91	59.62	56.28
2-1	Best	66.99	64.73	65.13	64.31	70.51	68.27	71.79	68.97	68.27	59.04	71.15	69.74	70.51	69.61
	Last	62.44	59.89	62.44	60.62	68.27	66.28	66.99	65.58	63.14	49.17	68.91	67.89	68.59	66.86
2-3	Best	75.90	74.31	74.74	71.56	78.85	76.35	81.41	77.37	72.76	70.06	82.05	77.18	80.45	78.59
	Last	71.67	70.13	70.58	69.04	76.60	73.72	80.13	74.49	68.91	59.10	77.24	73.21	78.85	75.38
3-0	Best	37.05	33.49	47.18	45.71	43.91	42.37	42.63	41.09	41.99	34.10	46.79	43.72	48.40	46.03
	Last	28.01	26.33	42.44	38.67	41.67	36.86	31.41	28.21	34.94	25.45	41.99	35.70	42.63	38.40
3-1	Best	52.56	49.35	57.31	56.30	64.42	62.63	64.74	62.88	59.94	46.60	63.46	61.60	63.78	61.99
	Last	39.74	37.10	52.95	51.23	60.26	58.91	62.18	59.62	49.36	36.73	63.14	59.68	60.90	58.59
3-2	Best	71.03	68.77	72.69	71.60	74.04	70.96	73.40	71.67	75.64	64.23	71.15	70.19	73.72	71.67
	Last	62.24	56.99	67.50	65.46	71.47	68.59	70.83	67.50	73.40	59.10	69.23	67.12	69.87	69.04
Best average		58.14	55.60	59.41	57.57	62.50	60.09	63.54	61.02	59.43	52.80	63.46	60.99	64.37	61.92
Last average		50.72	48.12	55.09	52.78	59.30	56.58	59.46	56.49	54.06	44.79	60.74	57.44	61.75	58.44
Best bias		0.00	0.00	1.27	1.97	4.36	4.49	5.32	5.39	1.29	-2.80	5.32	5.39	6.23	6.32
Last bias		0.00	0.00	4.37	4.66	8.57	8.46	10.02	9.32	3.34	-3.34	10.02	9.32	11.03	10.32

SEU with the time domain input

Task	Loc	Basis		AdaBN		MK-MMD		JMMD		CORAL		DANN		CDAN	
		Max	Mean	Max	Mean	Max	Mean	Max	Mean	Max	Mean	Max	Mean	Max	Mean
0-1	Best	48.91	48.33	52.93	51.59	57.04	53.81	57.04	53.14	45.45	38.80	54.84	51.32	57.77	53.40
	Last	42.70	39.18	49.82	47.69	54.40	48.65	53.81	45.98	35.78	27.57	44.72	41.61	55.28	46.48
1-0	Best	61.03	58.37	58.42	56.21	68.62	62.87	67.45	62.23	56.60	54.08	66.13	59.33	63.05	60.12
	Last	59.09	53.33	53.84	50.87	67.30	61.20	65.25	59.97	50.73	33.23	63.05	55.45	57.77	53.93
Best average		54.97	53.35	55.68	53.90	62.83	58.34	62.25	57.68	51.03	46.44	60.49	55.32	60.41	56.76
Last average		50.90	46.25	51.83	49.28	60.85	54.93	59.53	52.98	43.26	30.40	53.89	48.53	56.53	50.21
Best bias		0.00	0.00	0.71	0.55	7.86	4.99	7.28	4.33	-3.94	-6.91	5.52	1.97	5.44	3.41
Last bias		0.00	0.00	0.93	3.03	9.96	8.67	8.63	6.73	-7.64	-15.86	2.99	2.28	5.63	3.95

SEU with the frequency domain input

Task	Loc	Basis		AdaBN		MK-MMD		JMMD		CORAL		DANN		CDAN	
		Max	Mean	Max	Mean	Max	Mean	Max	Mean	Max	Mean	Max	Mean	Max	Mean
0-1	Best	37.36	34.61	41.99	36.35	42.96	40.38	46.92	44.90	53.37	38.39	47.07	43.02	49.41	41.58
	Last	27.74	22.89	24.99	20.68	39.00	33.14	43.11	36.28	30.94	25.13	44.57	34.63	41.64	32.34
1-0	Best	46.72	38.92	50.97	43.04	63.34	57.13	56.30	51.64	45.89	37.77	63.05	60.88	61.58	57.18
	Last	37.86	33.48	42.05	35.80	56.60	51.44	50.59	46.13	41.06	29.18	59.24	56.60	60.26	53.37
Best average		42.04	36.77	46.48	39.70	53.15	48.75	51.61	48.27	49.63	38.08	55.06	51.95	55.50	49.38
Last average		32.80	28.19	33.52	28.24	47.80	42.29	46.85	41.20	36.00	27.16	51.91	45.62	50.95	42.86
Best bias		0.00	0.00	4.44	2.93	11.11	11.99	9.57	11.50	7.59	1.31	13.02	15.18	13.46	12.62
Last bias		0.00	0.00	0.72	0.05	15.00	14.10	14.05	13.02	3.20	-1.03	19.11	17.43	18.15	14.67

PU-Types with the time domain input

Task	Loc	Basis		AdaBN		MK-MMD		JMMD		CORAL		DANN		CDAN	
		Max	Mean	Max	Mean	Max	Mean	Max	Mean	Max	Mean	Max	Mean	Max	Mean
0-1	Best	60.34	57.12	46.65	41.76	55.22	46.86	56.72	53.13	64.68	58.41	53.73	50.75	56.22	50.65
	Last	55.54	48.01	39.06	38.10	41.79	33.73	32.84	28.66	49.75	34.63	35.82	33.43	36.32	34.53
1-0	Best	50.40	46.32	74.27	69.95	49.33	44.53	58.67	54.67	54.00	42.13	57.33	54.40	58.67	56.27
	Last	34.13	33.79	68.40	61.71	36.67	32.13	47.33	37.73	33.33	33.33	40.67	35.20	38.67	35.47
Best average		55.37	51.72	60.46	55.85	52.28	45.70	57.70	53.90	59.34	50.27	55.53	52.57	57.45	53.46
Last average		44.84	40.90	53.73	49.90	39.23	32.93	40.09	33.20	41.54	33.98	38.25	34.32	37.50	35.00
Best bias		0.00	0.00	5.09	4.13	-3.10	-6.02	2.33	2.18	3.97	-1.45	0.16	0.85	2.07	1.74
Last bias		0.00	0.00	8.90	9.00	-5.61	-7.97	-4.75	-7.70	-3.30	-6.92	-6.59	-6.58	-7.34	-5.90

PU-Types with the time domain input

Task	Loc	Basis		AdaBN		MK-MMD		JMMD		CORAL		DANN		CDAN	
		Max	Mean	Max	Mean	Max	Mean	Max	Mean	Max	Mean	Max	Mean	Max	Mean
0-1	Best	62.54	44.78	49.95	41.56	46.77	46.57	45.77	41.29	67.66	59.50	54.73	49.35	44.78	42.79
	Last	36.86	33.63	38.26	36.80	45.27	42.19	33.83	33.04	39.30	35.02	45.77	45.47	44.78	37.51
1-0	Best	71.60	66.56	70.53	66.53	63.33	61.33	68.67	64.93	65.33	57.60	69.33	66.40	74.00	68.80
	Last	62.27	59.79	66.80	61.41	59.33	56.13	62.67	58.00	38.00	34.53	65.33	63.46	73.33	64.27
Best average		67.07	55.67	60.24	54.05	55.05	53.95	57.22	53.11	66.50	58.55	62.03	57.88	59.39	55.79
Last average		49.57	46.71	52.53	49.11	52.30	49.16	48.25	45.52	38.65	34.78	55.55	54.47	59.06	50.89
Best bias		0.00	0.00	-6.83	-1.62	-12.02	-1.72	-9.85	-2.55	-0.58	2.88	-5.04	2.21	-7.68	0.12
Last bias		0.00	0.00	2.96	2.40	2.74	2.45	-1.32	-1.19	-10.92	-11.93	5.99	7.76	9.49	4.18